

UNCLASSIFIED

AD NUMBER

AD858384

LIMITATION CHANGES

TO:

Approved for public release; distribution is unlimited.

FROM:

Distribution authorized to U.S. Gov't. agencies and their contractors;
Administrative/Operational Use; MAY 1969. Other requests shall be referred to Army Aviation Materiels Lab., Fort Eustis, VA.

AUTHORITY

USAAMRDL ltr 23 Jun 1971

THIS PAGE IS UNCLASSIFIED

**Best Available
Copy
for all Pictures**

AD858384

AD

USAALABS TECHNICAL REPORT 69-34

A STUDY TO DETERMINE IF A CORRELATION EXISTS
BETWEEN METAL FATIGUE LIFE AND THE
CAPABILITY OF THE METAL TO ABSORB
OR RETAIN AN INERT GAS

By

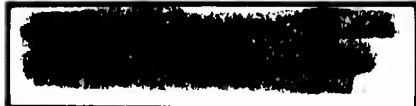
Albert J. Frasca

57 D C SEP 15 1969

May 1969

U. S. ARMY AVIATION MATERIEL LABORATORIES
FORT EUSTIS, VIRGINIA

CONTRACT DAAJ02-67-C-0021
INDUSTRIAL NUCLEONICS CORPORATION
COLUMBUS, OHIO



84

DEPARTMENT OF THE ARMY
U. S. ARMY AVIATION MATERIEL LABORATORIES
Fort Eustis, Virginia 23604

ERRATUM

USAAVLABS Technical Report 69-34

TITLE: A Study To Determine if a Correlation Exists Between Metal
Fatigue Life and the Capability of the Metal To Absorb or
Retain an Inert Gas

Delete the statement on cover, title page, and block 10 of DD Form 1473
which reads

"This document has been approved for public release and sale; its
distribution is unlimited."

and replace with the following statement:

"This document is subject to special export controls, and each
transmittal to foreign governments or foreign nationals may be
made only with prior approval of US Army Aviation Materiel
Laboratories, Fort Eustis, Virginia 23604."



DEPARTMENT OF THE ARMY
U. S. ARMY AVIATION MATERIEL LABORATORIES
FORT EUSTIS, VIRGINIA 23604

The effort reported herein is a part of a program to develop concepts of aircraft maintenance, inspection, and diagnostic equipment suitable for field application.

The report presents the results of a program to determine the feasibility of using the capability of a metal to absorb or retain an inert gas as a means for detecting impending fatigue failure.

This command concurs with the findings of the contractor.

Task 1F162203A43405
Contract DAAJ02-67-C-0021
USAAVLABS Technical Report 69-34
May 1969

A STUDY TO DETERMINE IF A CORRELATION EXISTS
BETWEEN METAL FATIGUE LIFE AND THE
CAPABILITY OF THE METAL TO ABSORB
OR RETAIN AN INERT GAS

Final Report

By

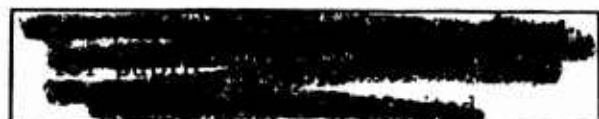
Albert J. Frasca

Prepared by

Industrial Nucleonics Corporation
Columbus, Ohio

for

U. S. ARMY AVIATION MATERIEL LABORATORIES
FORT EUSTIS, VIRGINIA



SUMMARY

The purpose of this study was to determine if a correlation exists between stressed metal fatigue and the ability of a metal to absorb or retain inert gas. Aluminum, stainless steel, and normalized steel samples were fatigued to percentages of their normal fatigue life and examined for preferential inert gas absorption in high fatigue regions. The inert gas was krypton, which was enriched with Kr-85, a radioactive tracer, for identification. The procedure was reversed for the same types of metals by allowing krypton absorption into the metals and examining for preferential release from subsequently fatigued areas. Autoradiography and radiometric analysis did not indicate any relationship between release or absorption of krypton and stress fatigue life with one exception; in the case of 4130 steel, limited results indicate that when Kr-85 absorption precedes fatigue, autoradiography and radiometric measurements can detect fatigue near failure. Peripheral results indicate that autoradiography is able to detect cracks in metals whether the inert gas absorption precedes or follows fatigue.

TABLE OF CONTENTS

	<u>Page</u>
SUMMARY	iii
LIST OF ILLUSTRATIONS	vii
LIST OF TABLES	x
LIST OF SYMBOLS	xi
1.0 INTRODUCTION	1
2.0 PROGRAM DESCRIPTION	1
3.0 PHASE A- PRELIMINARY DESIGN AND EVALUATION.....	2
3.1 Material Evaluation	2
3.2 Design and Fabrication of Specimens and Specimen Holder	4
3.3 Effect of Kryptonation on Fatigue Life	6
3.3.1 Mechanical Properties	6
3.3.2 Stress Level Definition	8
3.3.3 Population Comparison	8
3.4 Resultant Parameter Decisions	20
4.0 PHASE B - ABSORPTION AND RELEASE TESTING ..	20
4.1 Kr-85 Absorption	20
4.2 Kr-85 Release	34
4.2.1 Fatigue Process	35
4.2.2 Retention With Time	41
4.2.3 Retention Over Useful Cycle Life	62

	<u>Page</u>
4.2.4 Retention Near Failure	62
5.0 RESULTS AND CONCLUSIONS	69
6.0 DISTRIBUTION	71

LIST OF ILLUSTRATIONS

<u>Figure</u>		<u>Page</u>
1	Test Specimen	5
2	S-N Curve for AISI 4130 Steel (Normalized) . . .	12
3	S-N Curve for 2024-T3 Aluminum	13
4	S-N Curve for AISI 301 Half Hard Stainless Steel	14
5	Autoradiographs of Cracked 4130 Steel Specimens	26
6	Autoradiographs of Fatigued 2024 Aluminum Specimens (Max. Load, 30 ksi)	27
7	Autoradiographs of Fatigued 2024 Aluminum Specimens (Max. Load, 35 ksi)	28
8	Autoradiographs of Fatigued 2024 Aluminum Specimens (Max. Load, 45 ksi)	29
9	Autoradiographs of Fatigued 4130 Steel Specimens (Max. Load, 75 ksi)	30
10	Autoradiographs of Fatigued 4130 Steel Specimens (Max. Load, 87.5 ksi)	31
11	Autoradiographs of Fatigued 301 Stainless Steel Specimens (Max. Load, 108 ksi)	32
12	Autoradiographs of Fatigued 301 Stainless Steel Specimens (Max. Load, 117.5 ksi)	33
13	Activity Versus Fatigue Life for Stainless Steel Specimen	36
14	Activity Versus Fatigue Life for Stainless Steel Specimen	37

LIST OF ILLUSTRATIONS

<u>Figure</u>		<u>Page</u>
15	Activity Versus Fatigue Life for Stainless Steel Specimen	38
16	Autoradiographs of Fatigued 4130 Steel Specimen (Max. Load, 78 Ksi)	39
17	Autoradiographs of Fatigued 4130 Steel Specimens (Max. Load, 80 Ksi)	40
18	Autoradiographs of Fatigued 2024 Aluminum Specimens	42
19	Outgassing Curves of 2024 Aluminum Specimens	44
20	Outgassing Curves of 4130 Steel Specimens	45
21	Outgassing Curves of 301 Stainless Steel Specimens	46
22	Outgassing Curves of 2024 Aluminum Specimens	48
23	Outgassing Curves of 2024 Aluminum Specimens	49
24	Outgassing Curves of 2024 Aluminum Specimens	50
25	Outgassing Curves of 4130 Steel Specimens	54
26	Outgassing Curves of 4130 Steel Specimens	55
27	Outgassing Curves of 301 Stainless Steel Specimens	56
28	Outgassing Curves of 301 Stainless Steel Specimens	57

LIST OF ILLUSTRATIONS

<u>Figure</u>		<u>Page</u>
29	4130 Steel Specimens Tested to Fractions of Fatigue Life	63
30	301 Stainless Steel Specimens Tested to Fractions of Fatigue Life	64
31	Autoradiographs of 4130 Steel Specimen Near Failure	65
32	Autoradiographs of 4130 Steel Specimen Near Failure	66
33	Autoradiographs of 301 Stainless Steel Specimen Near Failure	67
34	Autoradiographs of 301 Stainless Steel Specimen Near Failure	68

LIST OF TABLES

<u>Table</u>		<u>Page</u>
I	Initial Kryptonation Data	3
II	Basic Mechanical Property Data for the Three Materials Being Studied	7
III	Summary of Completed Fatigue Tests of 4130 Normalized Steel	9
IV	Summary of Completed Fatigue Tests for 2024-T3 Aluminum	10
V	Summary of Completed Fatigue Tests for 301 Half Hard Stainless Steel	11
VI	301 Stainless Steel Fatigue Data	22
VII	4130 Steel Fatigue Data	23
VIII	2024-T3 Aluminum Fatigue Data	24
IX	2024-T3 Aluminum Retention Data (Max. Load, 30 Ksi)	51
X	2024-T3 Aluminum Retention Data (Max. Load, 35 Ksi)	52
XI	2024-T3 Aluminum Retention Data (Max. Load, 45 Ksi)	53
XII	4130 Steel Retention Data (Max. Load, 75 Ksi)	58
XIII	4130 Steel Retention Data (Max. Load, 87.5 Ksi)	59
XIV	301 Stainless Steel Retention Data (Max. Load, 75 Ksi)	60
XV	301 Stainless Steel Retention Data (Max. Load, 117.5 Ksi)	61

LIST OF SYMBOLS

A _i	2024-T3 aluminum specimen number i
D	absolute value of deviation of sample mean values assuming a logarithmic distribution
F	F statistic, equals ratio of sample variances
f(t)	statistical t-distribution
K _t	stress concentration factor
LCL	lower confidence limit
S	sample standard deviation
S _i ²	variance of sample i
S _k	4130 normalized steel specimen number k
S-N	stress versus number of cycles
SS _j	301 half hard stainless steel specimen number j
TUS	tensile ultimate strength
TYS	tensile yield strength
UCL	upper confidence limit
α	one minus confidence interval of decision
v	degrees of freedom
μ	arithmetic mean

BLANK PAGE

1.0 INTRODUCTION

The ability of a metal lattice to allow diffusion of gas into it is well known. Less well known is the ability of an inert gas to remain bound within the metal in contradiction to classical diffusion laws.¹ Inert gas which has been diffused in metal remains bound in the metal at a given temperature and tends to outgas from the metal as a function of temperature increases above the temperature of formation of the metal-inert gas composite. This study examined certain metals which had been impregnated with krypton gas for a correlation between the amount of krypton gas absorbed or retained in the metal and the stress fatigue history of the metal. The krypton retention or absorption was expected to be influenced by the lattice irregularities formed by stress fatiguing the metal. Krypton 85 was used as a radioactive tracer of the behavior of the host metal.

2.0 PROGRAM DESCRIPTION

The study involved two phases. The first phase required (1) design and fabrication of samples and experimental apparatus, (2) evaluation of several metals as to their ability to be sufficiently impregnated with Kr-85 gas for the purpose of the study, and (3) comparison of physical stress fatigue properties of unkryptonated and kryptonated metals used in the study.

The second phase of the study concerned the actual testing involved in determining whether a correlation exists between stressed metal fatigue and the absorption and retention of Kr-85. A group of specimens was first fatigued by a definite number of repetitions of a tensile stress. The number of fatigue cycles applied to the specimens was varied to cover the normal stress fatigue life of the metals at the stress level used. The specimens were subsequently kryptonated, and the correlation of Kr-85 absorption versus number of fatigue cycles was examined.

The reverse sequence of operations was also examined. Metal specimens were first kryptonated and subsequently fatigued over the normal stress fatigue life of the metal to examine Kr-85 release versus number of fatigue cycles.

¹ Chleck, D., Maehl, R., RADIOACTIVE KRYPTONATES - II PROPERTIES, Iter. J. Appl. Rad. and Is., Vol. 14, 1963, pp. 593-598.

Also, both sets of specimens were heated to allow the Kr-85 to outgas from the specimens. The curves of retention of Kr-85 in fatigued metal versus the time of heating and the retention of Kr-85 in unfatigued metal versus the time of heating were compared to examine if stress fatigue altered the binding of the Kr-85 in the metal lattice. Also, high spatial resolution autoradiography was used in both the absorption and release determinations to examine surface characteristics as a function of the number of fatigue cycles.

3.0 PHASE A- PRELIMINARY DESIGN AND EVALUATION

3.1 MATERIAL EVALUATION

Of six metals initially proposed as applicable to Army systems, three were to be chosen based on their ability to be kryptonated to suitable activity levels for analysis. The metals considered were three aluminum alloys (6061, 7075, and 2024) and three steel alloys (9310 case hardened, 301 stainless, and 321 stainless). All the materials were obtainable in a desirable initial form, except 9310 case hardened steel. Since reworking the 9310 would change its mechanical properties, it was not used. A suitable alternative to 9310 case hardened was found to be 4130 normalized steel.

Specimens of the six metals were made with a physical size of 3/4 inch in diameter and 1/8 inch in thickness. Two kryptonations were made using the six metals in each. The first test kryptonation was done at high temperature (572°F) and high pressure (800 psia), and for a duration of 16 hours. Since the activity concentration was considerably greater than that necessary for good statistical counting accuracy, a second kryptonation was made with suitable adjustment of the kryptonation parameters. The second kryptonation was done with a temperature of 300°F, with a pressure of 500 psia, and for a duration of 1 hour. Specimen count rates in counts per minute or Cpm as measured by a 1-inch end window GM tube are shown in Table I for the two kryptonations.

Based on these results, three materials were selected: 2024-T3 aluminum, 301 half hard stainless steel, and 4130 normalized steel. Since the lower temperature kryptonation was more than adequate for good counting statistics and since the mechanical properties of metals are related to the temperature history of a metal, 300°F was used in subsequent aluminum specimen kryptonations and 500°F for all steel specimens. These temperatures and the duration at these temperatures were such

TABLE I. INITIAL KRYPTONATION DATA

SPECIMEN KRYPTONATION NO. 1
 572°F , 16 Hours, 800 psi

Specimen	Activity (Cpm)
7075 Al	206,687
2024 Al	166,854
6061 Al	31,978
4130 Steel	58,196
301 Steel	12,918
321 Steel	10,526

Specimen	Activity (Cpm)
7075 Al	698
2024 Al	188
6061 Al	83
4130 Steel	1948
301 Steel	128
321 Steel	60

that mechanical properties of the chosen materials were not significantly changed. The particular metals chosen were based both on the ability of the metals to be kryptonated and on their applicability to Army systems.

3.2 DESIGN AND FABRICATION OF SPECIMENS AND SPECIMEN HOLDER

The design of the fatigue specimen was based on several experimental factors. A notched specimen shape was used to localize the fatigue deformation process by centralizing maximum stress within the notched region. This restricted the area to be investigated for changes in Kr-85 levels. The specimen's physical dimensions are shown in Figure 1. All specimens had a nominal 1/8-inch thickness. The stress concentration factor K_t , which is the factor by which an applied tension is multiplied to obtain the stress at the notched region, was 1.36 for all specimens. The specimen's flat design was selected because it would assure reproducible counting geometry in the radioactivity detection system used.

A fatigue specimen holder for a kryptonation vessel was constructed to allow efficient kryptonation of a large number of specimens. Since over 200 fatigue specimens were to be examined, the holder was designed to house 73 specimens at one time. The ability to kryptonate such a large quantity of specimens not only reduced the total time involved in kryptonation but also assured kryptonation levels which were as uniform as constant kryptonation parameters allow. The upper limit of 73 specimens was fixed by experimental limitations. If all 200 had been kryptonated at once, the pressure attainable would have been too low for significant activity levels. As the specimens' activity concentration depends on the Kr-85 gas pressure and since this pressure is reduced with any increase in the unfilled volume of the kryptonation vessel, the free volume was required to be minimum to obtain high activity concentrations. All holes and notched regions in the specimens were filled with machined metal fillers to minimize this free volume.

As the specimens were stacked like a deck of cards on edge in the pressure vessel, the minimum spacing between specimens to obtain uniform kryptonation levels and least free volume was of interest. To maintain gas pressure concentrations on the specimen surface, it was only necessary that the spacing between blades be significantly wider than the mean free path between collisions of the gas atoms (Kr-85 is a monoatomic gas). For example, at a pressure of 100 psia and a temperature of 300°F, the mean free path of Kr-85 gas atoms is 10^{-5} inch. Since the mean free path decreases with increased pressure when the number of atoms is constant and a pressure of 180 psia was used in the

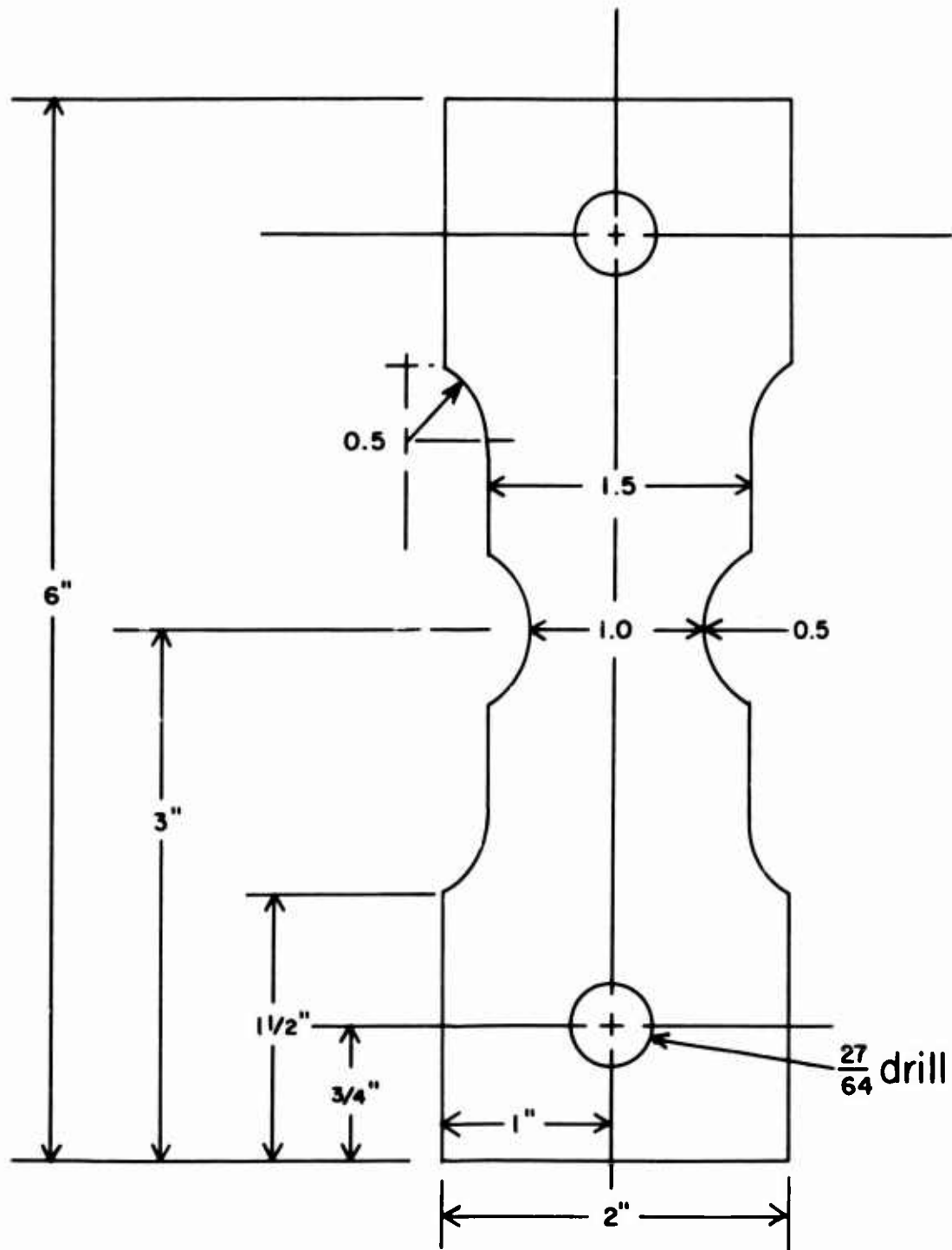


Figure 1. Test Specimen.

kryptonations, a specimen surface spacing of one mil (100 times the mean free path at 100 psia) was used and was adequate for the pressures and temperatures used.

3.3 EFFECT OF KRYPTONATION ON FATIGUE LIFE

To examine whether the kryptonation process had any effect on the fatigue life of the metals studied, the following test program was carried out:

- (1) Five kryptonated and five unkryptonated specimens of each metal were fatigue tested to failure to determine by statistical analysis whether the kryptonation process adversely affected a metal's fatigue life.
- (2) Five kryptonated specimens of each material were fatigue tested at various stress levels until failure to provide an S-N fatigue endurance curve. This information was used to determine the appropriate stress levels for subsequent fatigue testing.

The parameters used in this kryptonation to determine the activity level obtained were a pressure of 140 psia, a temperature of 300° F, and a duration of 16 hours. Following kryptonation, Battelle Memorial Institute carried out mechanical property tests as listed below:

- (1) Performed tensile tests on four specimens of each of the three materials to obtain basic mechanical property data.
- (2) Obtained S-N curves for the 2024-T3 aluminum, the 301 half hard stainless steel, and the 4130 normalized steel.
- (3) Analyzed the statistical variation in fatigue life of the three unkryptonated materials at one stress level.
- (4) Analyzed the statistical variation in fatigue life of the same three kryptonated materials at the same respective stress level where fatigue lives of unkryptonated specimens were analyzed.
- (5) Compared the results of the statistical analysis of the kryptonated specimens with those of the unkryptonated ones.

3.3.1 Mechanical Properties

The basic mechanical property data are presented in Table II for each material. In the table, the average of four specimens is given for tests of tensile yield strength, tensile ultimate strength, and elongation.

TABLE II. BASIC MECHANICAL PROPERTY
DATA FOR THE THREE
MATERIALS BEING STUDIED

Specimen Number	Tensile Yield Strength (Ksi)	Tensile Ultimate Strength (Ksi)	Elongation (percent in 2 inches)
<u>4130 Normalized Steel</u>			
1	83.3	104.5	18.5
2	82.6	104.3	18.5
3	83.0	104.5	18.5
4	83.4	104.5	18.5
Average value	83.1	104.5	18.5
<u>301 Half Hard Stainless Steel</u>			
1	124.5	158.5	31.0
2	125.2	157.5	32.0
3	124.8	158.0	30.0
4	125.6	159.4	34.0
Average value	125.0	158.3	31.8
<u>2024-T3 Aluminum</u>			
1	56.2	71.4	19.5
2	54.0	71.7	20.0
3	54.0	71.7	20.0
4	54.4	72.3	19.5
Average value	54.7	71.8	19.8

The determined values of ultimate tensile strength were used in conjunction with reference information² in the selection of stress loads for the fatigue tests.

3.3.2 Stress Level Definition

The data from the completed tests are summarized in Tables III, IV, and V and plotted in Figures 2, 3, and 4. For each material, a table indicates the actual cycle lifetime before failure at stress levels giving a lifetime range of 10^4 to 10^7 cycles. The tensile yield strength, TYS, and tensile ultimate strength, TUS, are given in the tables. These tabulated data were used to derive the S-N curve for each material; i. e., Figures 2, 3, and 4. After examining each S-N curve, stress levels which would span the minimum slope region of the S-N curve for each material were chosen for statistical analysis of fatigue life. These data at a fixed stress level in a specific table compare the number of cycle lifetimes of five kryptonated and five unkryptonated specimens to allow statistical examination of their respective populations. The fatigue life of metal is well approximated by a log normal distribution, and the latter distribution was assumed in determining the average number of cycles for fatigue failure found in each table.

3.3.3 Population Comparison

From the mean and standard deviation, as calculated using the log normal distribution, 90 percent confidence intervals on the mean life were computed and are indicated in Figures 2, 3, and 4. To compare the variances and average length of the fatigue lives of the kryptonated specimens and unkryptonated specimens, F-tests were performed on the variances and t-tests were performed on the mean fatigue lives of comparative data of each metal. The analysis, with sample computations and necessary definitions, is briefly given in the following.

Assume: The cyclic fatigue lives are log normally distributed.

Definition:

$$(1) \text{ Mean specimen life, } \overline{\ln N_f} = \sum_{i=1}^n \ln N_{f,i} / n$$

where N_f is kilocycles to failure
and n is number of specimens in sample.

² METALLIC MATERIALS AND ELEMENTS FOR AEROSPACE VEHICLE STRUCTURES, MIL-HDBK-5A, 1966, Feb. 8, D. O. D.

TABLE III. SUMMARY OF COMPLETED FATIGUE
TESTS OF 4130 NORMALIZED STEEL

Specimen Number	Maximum Nominal Stress (psi)	Cycles to Failure	Results
<u>Unkryptonated</u>			
S2	105,000	38,100	
S3	97,000	79,700	
S4	90,000	138,800	
S39	85,000	166,500	
S38	77,500	183,800	TUS = 104,500 psi
S40	76,000	>14,125,300	
S6	75,000	>10,550,000	TYs = 83,800 psi
<u>Average Cycles to Failure</u>			
S5	80,000	204,600	
S92	80,000	152,600	
S93	80,000	182,500	321,200 (assuming
S94	80,000	184,400	a log normal
S96	80,000	3,250,500	distribution)
<u>Kryptonated</u>			
<u>Average Cycles to Failure</u>			
S13	80,000	>10,006,700	
S14	80,000	1,066,000	
S15	80,000	941,500	1,006,100
S18	80,000	318,000	(assuming a log
S19	80,000	323,000	normal distribution)

TABLE IV. SUMMARY OF COMPLETED FATIGUE TESTS FOR 2024-T3 ALUMINUM

Specimen Number	Maximum Nominal Stress (psi)	Cycles to Failure	Results
<u>Unkryptonated</u>			
A1	63,600	11,700	
A2	42,000	88,700	
A4	35,000	180,700	
A17	35,000	4,460,000	TUS = 71,800 psi
A8	33,000	6,140,000	
A5	32,500	180,700	TYS = 54,700 psi
A7	32,000	7,353,600	
A6	31,000	9,833,400	
A3	30,000	>10,597,000	
<u>Average Cycles to Failure</u>			
A87	38,000	146,700	
A97	38,000	158,700	220,700 (assuming
A98	38,000	153,100	a log normal
A99	38,000	208,300	distribution)
A100	38,000	704,500	
<u>Kryptonated</u>			
<u>Average Cycles to Failure</u>			
A4	38,000	158,800	
A13	38,000	4,496,400	
A54	38,000	159,700	391,300 (assuming
A58	38,000	281,500	a log normal
A59	38,000	285,700	distribution)

TABLE V. SUMMARY OF COMPLETED FATIGUE
TESTS FOR 301 HALF HARD
STAINLESS STEEL

Specimen Number	Maximum Nominal Stress (psi)	Cycles to Failure	Results
<u>Unkryptonated</u>			
SS66	130,000	30,080	
SS31	120,000	41,060	
SS37	120,000	45,990	
SS38	117,500	39,040	TUS = 158,400 psi
SS35	116,000	39,600	
SS34	114,000	970,660	TYS = 125,000 psi
SS45	112,000	26,600	
SS85	108,000	>6,989,100	
SS33	100,000	>6,719,100	
<u>Average Cycles to Failure</u>			
SS32	115,000	8,406,340	
SS36	115,000	1,713,810	299,000 (assuming
SS39	115,000	50,400	a log normal
SS41	115,000	53,950	distribution)
SS86	115,000	60,850	
<u>Kryptonated</u>			
<u>Average Cycles to Failure</u>			
SS4	115,000	103,610	
SS10	115,000	71,420	96,700 (assuming
SS15	115,000	386,760	a log normal
SS16	115,000	54,390	distribution)
SS26	115,000	54,280	

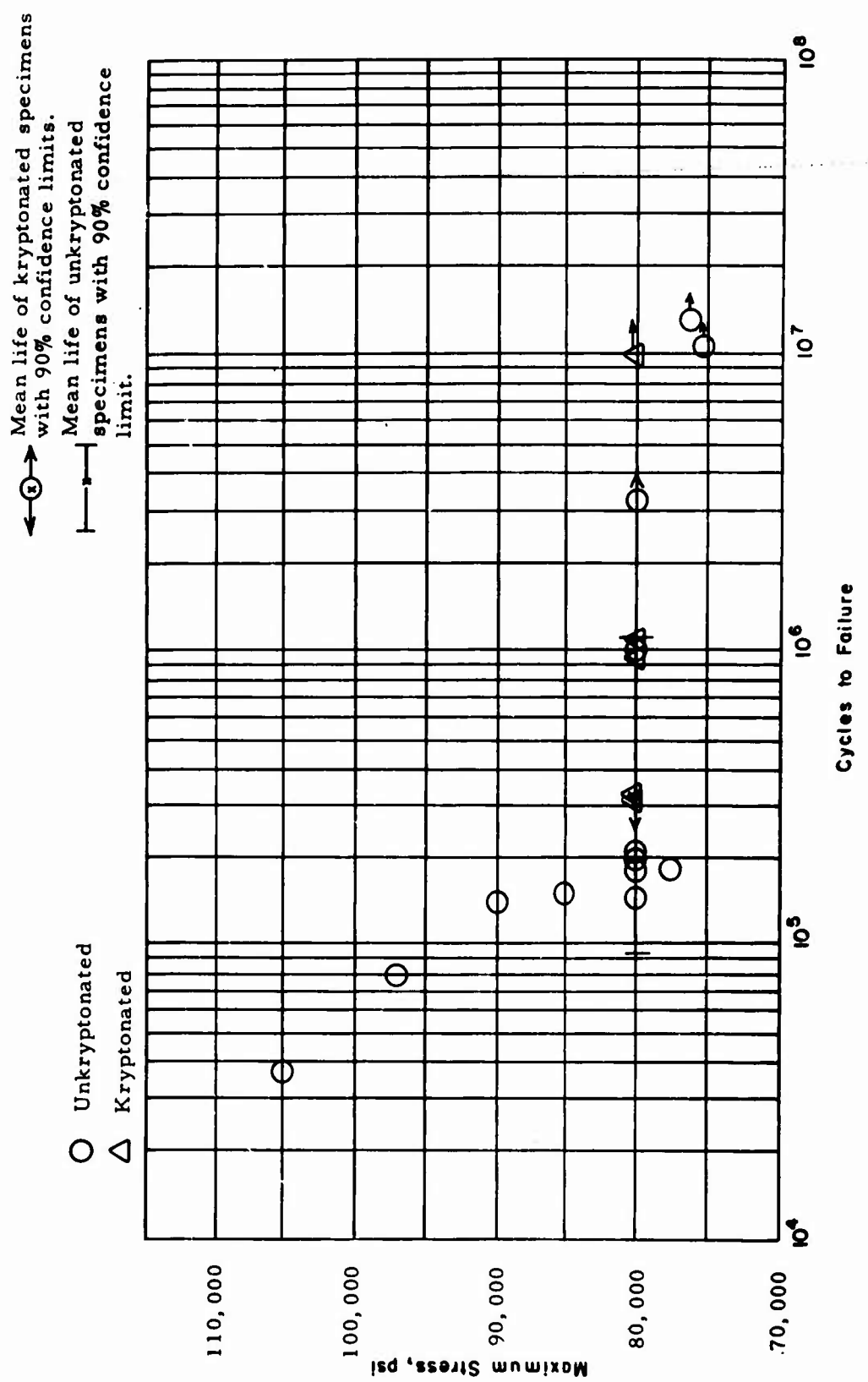


Figure 2. S-N Curve for AISI 4130 Steel (Normalized).

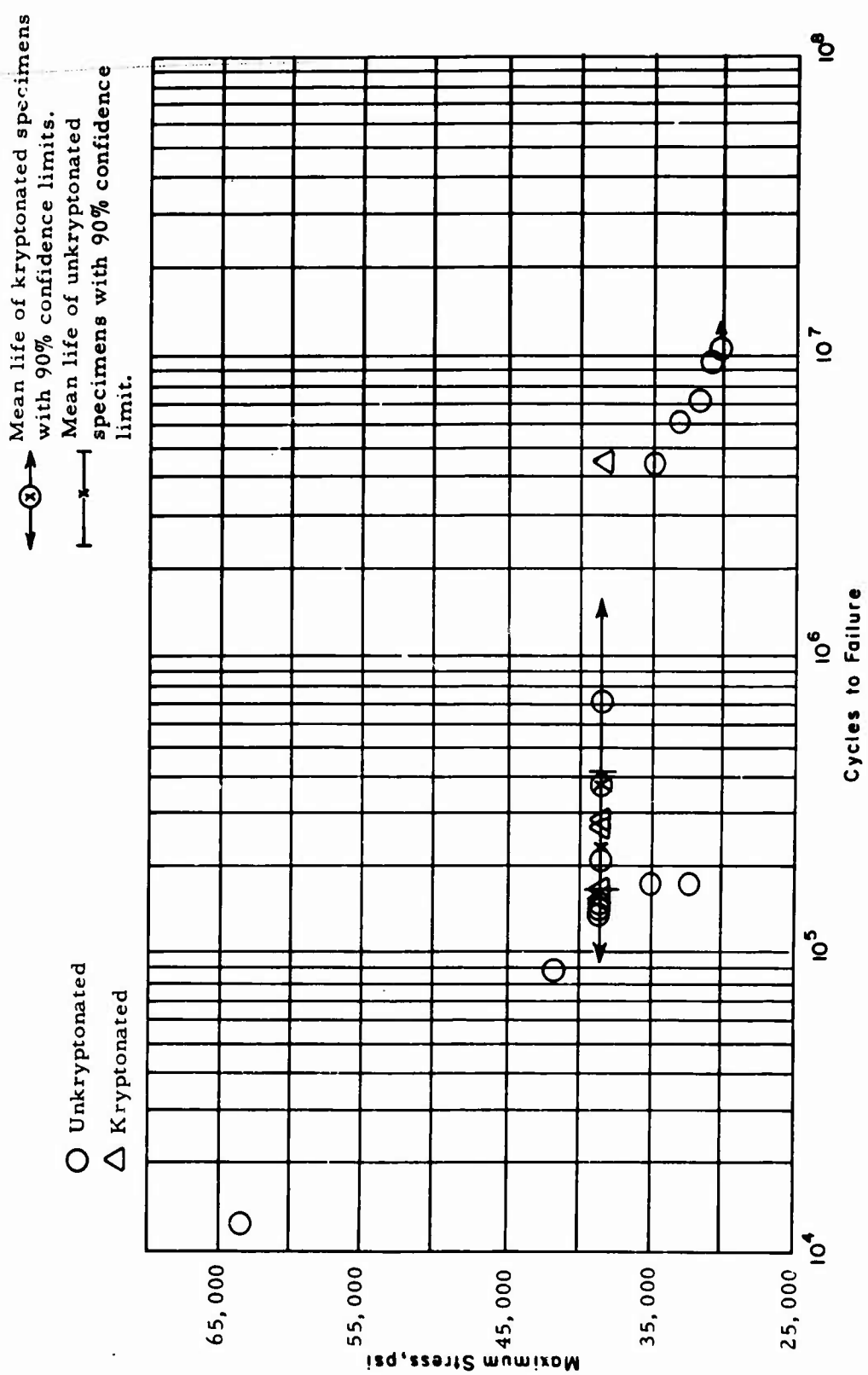


Figure 3. S-N Curve for 2024-T3 Aluminum.

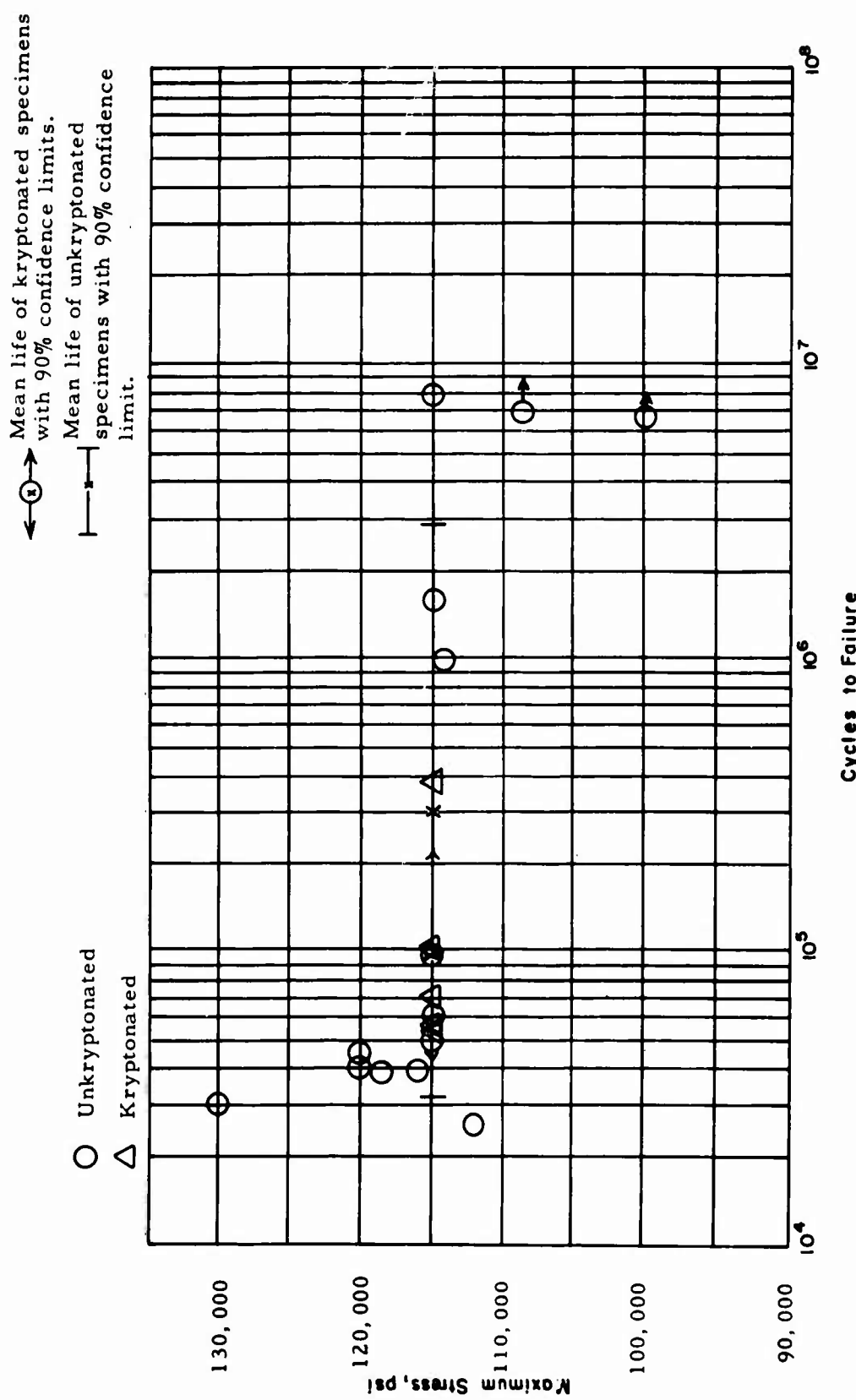


Figure 4. S-N Curve for AISI 301 Half Hard Stainless Steel.

$$(2) \text{ The sample standard deviation, } S \equiv \left[\frac{n \sum_{i=1}^n \ln N_{f_i}^2 - \left(\sum_{i=1}^n \ln N_{f_i} \right)^2}{n(n-1)} \right]^{1/2}$$

(3) Then, a " $1 - \alpha$ " confidence interval for the mean, μ , can be shown to be:

$$\overline{\ln N_f} - t_{\alpha/2} S_n^{-1/2} < \mu < \overline{\ln N_f} + t_{\alpha/2} S_n^{-1/2}$$

where $\alpha = \int_{t_\alpha}^{\infty} f(t) dt$ and $f(t)$ is the t-distribution for $\nu (= n-1)$ degrees of freedom.

(4) The F-test; if F is not in the closed interval from $1/F_{\alpha/2}$ to $F_{\alpha/2}$, then the samples' variances are different at a significant level of α ,

$$\text{where } F = S_A^2 / S_B^2.$$

S_A^2 and S_B^2 are the variances of samples A and B, respectively,

$F_{\alpha/2}$ is the "F-statistic",

$$F_{\alpha/2} = F_{\alpha/2}(\nu_A, \nu_B) \text{ for}$$

$\nu_A (= n_A - 1)$ and $\nu_B (= n_B - 1)$ degrees of freedom,

and n_A and n_B are the number of specimens in samples A and B, respectively.

(5) The "t-test"; if $D > u$, then samples A and B differ in average

$$\text{where } D = \left| \frac{\ln N_f}{n_A} - \frac{\ln N_f}{n_B} \right|,$$

$$u = t_{\alpha/2} S_p \left\{ \frac{n_A + n_B}{n_A n_B} \right\}^{1/2},$$

$t_{\alpha/2}$ is the "t-statistic" with $(n_A + n_B - 2)$ degrees of freedom,

and

$$S_p = \left\{ \frac{(n_A - 1) S_A^2 + (n_B - 1) S_B^2}{n_A + n_B - 2} \right\}^{1/2}$$

4130 Steel At 80 KSI Maximum Stress

Sample A - Unkryptonated

$$\frac{\ln N_f}{n_A} = \frac{28.859}{5} = 5.772^*$$

$$S_A = 1.298, 1 - \alpha = 0.90, t_{\alpha/2} = t_{0.05} = 2.132^3$$

$$t_{\alpha/2} S_A n_A^{-1/2} = 1.238$$

$$\text{mean, } \mu, = \exp \left(\frac{\ln N_f}{n_A} \right) = 321,100 \text{ cycles}$$

$$\text{lower confidence limit, LCL,} = \exp \left(\frac{\ln N_f}{n_A} - t_{\alpha/2} S_A n_A^{-1/2} \right) = 93,100 \text{ cycles}$$

$$\text{upper confidence limit, UCL,} = \exp \left(\frac{\ln N_f}{n_A} + t_{\alpha/2} S_A n_A^{-1/2} \right) = 1,107,100 \text{ cycles}$$

*For computational convenience, these numbers are natural logarithms of kilocycles.

³Miller, Irwin, Freund, J. E., PROBABILITY AND STATISTICS FOR ENGINEERS, Prentice Hall, Inc., New Jersey, 1965, Table IV, p. 399.

Sample B - Kryptonated

$$\overline{\ln N_{f_B}} = 6.9138; S_B = 1.4053$$

$$\mu = 1,006,100 \text{ cycles}$$

$$LCL = 263,400 \text{ cycles}$$

$$UCL = 3,842,200 \text{ cycles}$$

Comparison of Samples A and B

$$F = S_A^2 / S_B^2 = (1.298 / 1.4053)^2 = 0.853$$

At significance level $\alpha = 0.10$

$$F_{\alpha/2} (\nu_A, \nu_B) = F_{0.05} (4, 4) = 6.39^4$$

$$1/F_{\alpha/2} = 0.156.$$

Now, $0.156 < 0.853 < 6.39$; therefore, we conclude no significant difference in variance.

$$D = |5.772 - 6.9138| = 1.142$$

$$S_p = \left\{ \frac{4(1.298)^2 + 4(1.405)^2}{8} \right\}^{1/2} = 1.35$$

if $\alpha = 0.10$, $t_{\alpha/2} = 1.860$ and

$$u = (1.860) (1.35) \left(\frac{10}{25} \right)^{1/2} = 1.59,$$

Now, $1.14 < 1.59$; therefore, we conclude no significant difference in average strength between the kryptonated and nonkryptonated specimens of 4130 steel.

⁴Op. cit., Miller, Freund, Table VIa, p. 401.

2024-T3 Aluminum at 38 Ksi Maximum Stress

Sample A - Unkrytonated

$$\overline{\ln N_f}_A = 5.397; S_A = 0.663$$

$$\mu = 220,700 \text{ cycles}$$

$$LCL = 117,300 \text{ cycles}$$

$$UCL = 415,300 \text{ cycles}$$

Sample B - Krytonated

$$\overline{\ln N_f}_B = 5.969; S_B = 1.395$$

$$\mu = 391,300 \text{ cycles}$$

$$LCL = 103,400 \text{ cycles}$$

$$UCL = 1,478,800 \text{ cycles}$$

Comparison of Samples A and B

$$F = 0.226$$

$$\text{At } \alpha = 0.10; F_{\alpha/2} = 6.39, 1/F_{\alpha/2} = 0.156.$$

Now, $0.156 < 0.226 < 6.39$; therefore, we conclude no significant difference in variance.

$$D = 0.572; \text{ at } \alpha = 0.10, u = 1.28.$$

Now, $0.572 < 1.28$; therefore, we conclude no significant difference in average strength.

301 Half Hard Stainless Steel at 115 Ksi Maximum Stress

Sample A - Unkrytonated

$$\overline{\ln N_f}_A = 5.700; S_A = 2.388$$

μ = 299,000 cycles

LCL = 30,700 cycles

UCL = 2,913,200 cycles

Sample B - Kryptonated

$\overline{\ln N_{f_B}}$ = 4.5718; S_B = 0.8170

μ = 96,700 cycles

LCL = 44,400 cycles

UCL = 210,800 cycles

Comparison of Samples A and B

$F = 8.5433$

at $\alpha = 0.10$; $F_{\alpha/2} = 6.39$, $1/F_{\alpha/2} = 0.156$.

Now, $8.543 > 6.39$; therefore, variances of samples are significantly different.

At $\alpha = 0.05$, however, $F_{\alpha/2} = 9.60$, $1/F_{\alpha/2} = 0.104$.

Now, $0.104 < 8.543 < 9.60$; therefore, at this level the variances are not significantly different.

$D = 1.128$; at $\alpha = 0.10$, $u = 2.010$

Now, $1.128 < 2.010$; therefore, the two samples do not differ in average strength.

In summary of this analysis, samples A and B belong to different populations only if either their means or their variances differ significantly, since a normal distribution is characterized by its mean and variance or standard deviation. For the 4130 normalized steel at 80 ksi maximum stress and the 2024-T3 aluminum at 38 ksi maximum stress, the F- and t-tests at 90 percent confidence levels showed no significant difference between the mean lives and variances of the kryptonated and unkryptonated populations. For the 301 half hard stainless steel at 115 ksi maximum stress, the F-test at 90 percent confidence showed a significant difference between the variance of the unkryptonated and kryptonated populations; however, at 95 percent confidence, the difference was not significant. The t-test at 90 percent confidence showed no significant difference in mean life. Our conclusion is that kryptonation did not significantly alter the fatigue lives of these three metals at the stress levels investigated.

3.4 RESULTANT PARAMETER DECISIONS

From these results, decisions were made concerning stress levels to apply in the absorption and release aspects of the study. To obtain various conditions of fatigue damage for radiometric analysis of kryptonated samples, three stress levels were selected for each material. As indicated by each material's S-N curve (Figures 2, 3, and 4), stress levels were selected to yield average fatigue lives of 10^5 , 10^6 , and 10^7 cycles. The stress levels corresponding to these fatigue lives were:

- (1) 45, 35, and 30 ksi maximum stress for the 2024-T3 aluminum (Figure 3).
- (2) 87.5, 78, and 75 ksi maximum stress for the 4130 normalized steel (Figure 2).
- (3) 117.5, 112.5 and 108 ksi maximum stress for the 301 half hard stainless steel (Figure 4).

4.0 PHASE B - ABSORPTION AND RELEASE TESTING

4.1 Kr-85 ABSORPTION

The specimens involved in this portion of the study were stress fatigued to sample the average fatigue life of the metals at stress levels indicated in Section 3.4 of this report. Following this, the specimens

were kryptonated and radiometrically examined for correlation of Kr-85 absorption and the fatigue history of the specimens. The specific test examination was as follows:

- (1) Twenty-four specimens of each unkryptonated steel (4130 steel and 301 stainless steel) were fatigue tested for six different number of cycles to cover the average stress fatigued life span (10^1 , 10^2 , 10^3 , 10^4 , 10^5 , and 10^6 cycles) at two different stress levels. This meant that duplicate specimens were available at each of the latter number of fatigue cycles and at each stress level.
- (2) Fifty-four specimens of 2024 unkryptonated aluminum were fatigue tested for six different number of cycles at three different stress levels. This meant that triplicate specimens were available at each of the latter number of fatigue cycles and at each stress level.
- (3) The specimens from (1) and (2) and six control specimens of each material were kryptonated with the following parameters: 500°F , 21 hours, and 140 psi for the steel specimens; and 300°F , 22 hours, and 100 psi for the aluminum specimens.
- (4) The correlation of the 120 specimens' absorption and the stress fatigue history of the specimens were examined using radiometric and autoradiographic measurements.
- (5) Autoradiographs were made of the specimens in Section (4), and the correlation between autoradiographic features and fatigue history was investigated.

The results of the fatigue cycling and subsequent kryptonation levels observed from specimens over the average life are given in Tables VI, VII, and VIII. Examination of the tabled data with reference to the correlation of Kr-85 concentration and the number of fatigue cycles indicates that no correlation was observed in these measurements. When the entire fatigued region was measured, as is implicitly done when radiometrically measured, no fatigue correlation was found.

Autoradiographs remove the ambiguity of an integral measurement by indicating any nonuniformities of activity concentration on the surface. Autoradiographs of 2024-T3 aluminum, 4130 normalized steel, and 301 half hard stainless steel specimens which had been fatigued over their average life at stress levels chosen from Subsection 3.4 are shown in Figures 5 through 12. Inspection of the area of higher stress, the notched region, revealed no noticeable change in krypton intensity with

TABLE VI. 301 STAINLESS STEEL FATIGUE DATA

Specimen Number	Max. Load (Ksi)	Number of Cycles	Specimens Cracked	Krypton Intensity (Cpm Coded Side/Cpm Uncoded Side)
SS67	117.5	7	No	441/429
SS68	117.5	7	No	326/437
SS69	117.5	47	No	382/294
SS70	117.5	47	No	460/504
SS71	117.5	325	No	416/323
SS72	117.5	325	No	332/485
SS73	117.5	2,250	No	385/452
SS74	117.5	2,250	No	463/337
SS75	117.5	14,680	No	275/417
SS76	117.5	14,680	No	739/573
SS77	117.5	38,900	Yes	357/351
SS78	117.5	42,130	Yes	289/338
SS79	108	15	No	442/374
SS80	108	15	No	470/572
SS81	108	220	No	425/697
SS82	108	220	No	358/457
SS83	108	3,025	No	990/1279
SS84	108	3,025	No	847/899
SS87	108	46,420	No	262/398
SS88	108	46,420	No	454/422
SS89	108	54,420	No	314/401
SS90	108	54,420	No	342/443
SS91	108	329,450	Yes	276/686
SS92	108	5,000,000	No	382/705

TABLE VII. 4130 STEEL FATIGUE DATA

Specimen Number	Max. Load (Ksi)	Number of Cycles	Specimens Cracked	Krypton Intensity (Cpm Coded Side/Cpm Uncoded Side)
S41	87.5	7	No	305/717
S42	87.5	7	No	269/324
S43	87.5	47	No	344/633
S44	87.5	47	No	238/390
S45	87.5	325	No	215/301
S46	87.5	325	No	619/239
S47	87.5	2,250	No	679/379
S48	87.5	2,250	No	305/264
S49	87.5	14,680	No	295/203
S50	87.5	14,680	No	108/750
S51	87.5	50,000	Yes	275/465
S52	87.5	29,400	Yes	287/563
S53	75	15	No	308/782
S54	75	15	No	228/311
S55	75	220	No	3753/301
S56	75	220	No	817/339
S57	75	3,025	No	213/248
S58	75	3,025	No	383/312
S59	75	46,420	No	369/439
S60	75	46,420	No	856/357
S61	75	681,250	No	305/343
S62	75	681,250	No	375/362
S63	75	256,000	Yes	385/293
S64	75	5,000,000	No	325/589

TABLE VIII. 2024-T3 ALUMINUM FATIGUE DATA

Specimen Number	Max. Load (Ksi)	Number of Cycles	Specimens Cracked	Krypton Intensity (Cpm Coded Side/Cpm Uncoded Side)
A18	45	7	No	3731/3693
A19	45	7	No	4613/3580
A20	45	7	No	4576/4776
A21	45	47	No	3690/4925
A22	45	47	No	4842/6775
A23	45	47	No	3416/4319
A24	45	325	No	2873/3636
A25	45	325	No	4918/4106
A26	45	325	No	2748/5003
A27	45	2,250	No	4797/5085
A28	45	2,250	No	3431/5187
A29	45	2,250	No	6471/4908
A30	45	14,680	No	6214/4378
A31	45	14,680	No	4556/5281
A32	45	14,680	No	6382/4430
A33	45	50,000	No	4675/5854
A34	45	50,000	No	5228/4707
A35	45	50,000	No	4499/4279
A36	35	10	No	3604/4588
A37	35	10	No	3488/3493
A38	35	10	No	4305/6013
A39	35	100	No	3584/5526
A40	35	100	No	5402/5163
A41	35	100	No	5085/3016
A42	35	100	No	6247/7621
A43	35	100	No	5369/4606
A44	35	1,000	No	4001/3679
A45	35	1,000	No	3386/3881
A46	35	1,000	No	4698/4701
A47	35	10,000	No	3027/3136
A48	35	10,000	No	4921/3485
A49	35	10,000	No	4929/5632
A50	35	10,000	No	3946/3377
A51	35	500,000	No	4468/5424
A52	35	500,000	No	3957/5293
A53	35	500,000	No	4681/4270

TABLE VIII - Continued

Specimen Number	Max. Load (Ksi)	Number of Cycles	Specimens Cracked	Krypton Intensity (Cpm Coded Side/Cpm Uncoded Side)
A68	30	15	No	2630/4344
A69	30	15	No	4844/4305
A70	30	15	No	3003/4408
A71	30	220	No	2473/3912
A72	30	220	No	2470/4198
A73	30	220	No	3452/2366
A74	30	3,025	No	3825/4758
A75	30	3,025	No	3552/2484
A76	30	3,025	No	5091/4514
A77	30	46,420	No	3925/4487
A78	30	46,420	No	3489/4384
A79	30	46,420	No	3417/5246
A80	30	681,250	No	3911/4736
A81	30	681,250	No	5328/3628
A82	30	681,250	No	3651/3893
A83	30	5,000,000	No	2671/3941
A84	30	5,000,000	No	4011/4935
A85	30	5,000,000	No	3429/4561
A14	Control	0	No	7769/5500
A62	Control	0	No	7566/7343
A63	Control	0	No	6373/9082

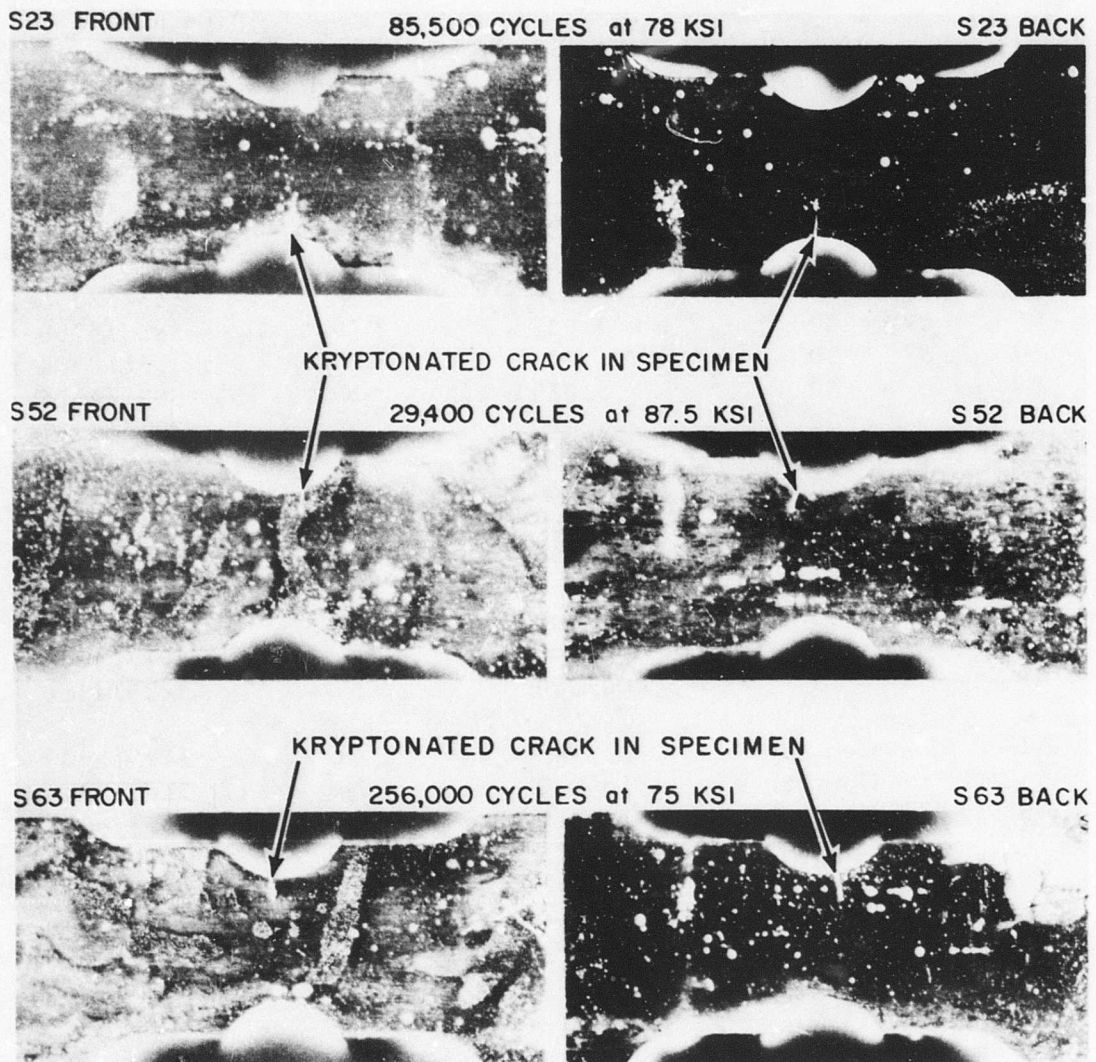


Figure 5. Autoradiographs of Cracked 4130 Steel Specimens.

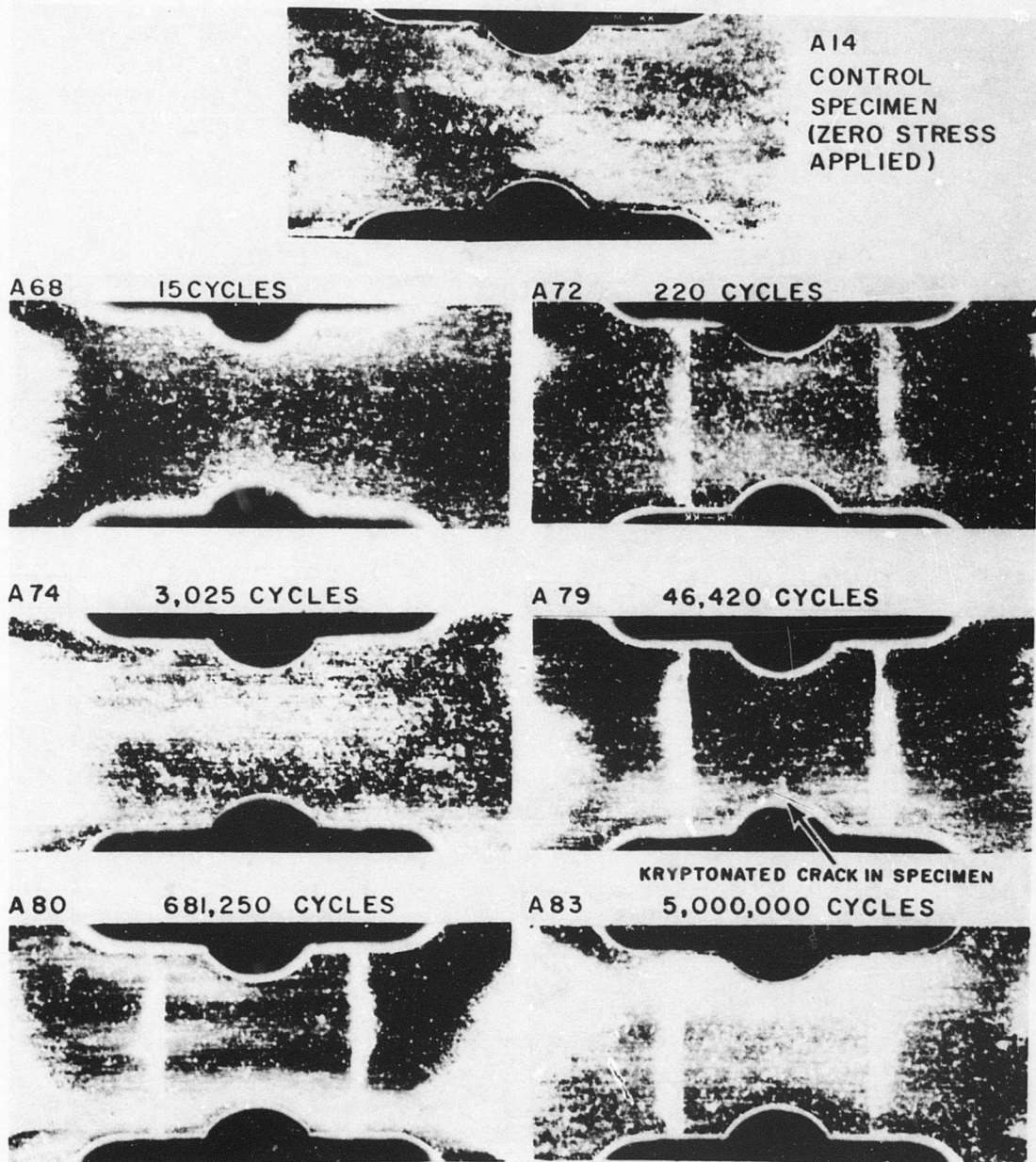


Figure 6. Autoradiographs of Fatigued 2024 Aluminum Specimens (Max. Load, 30 Ksi).

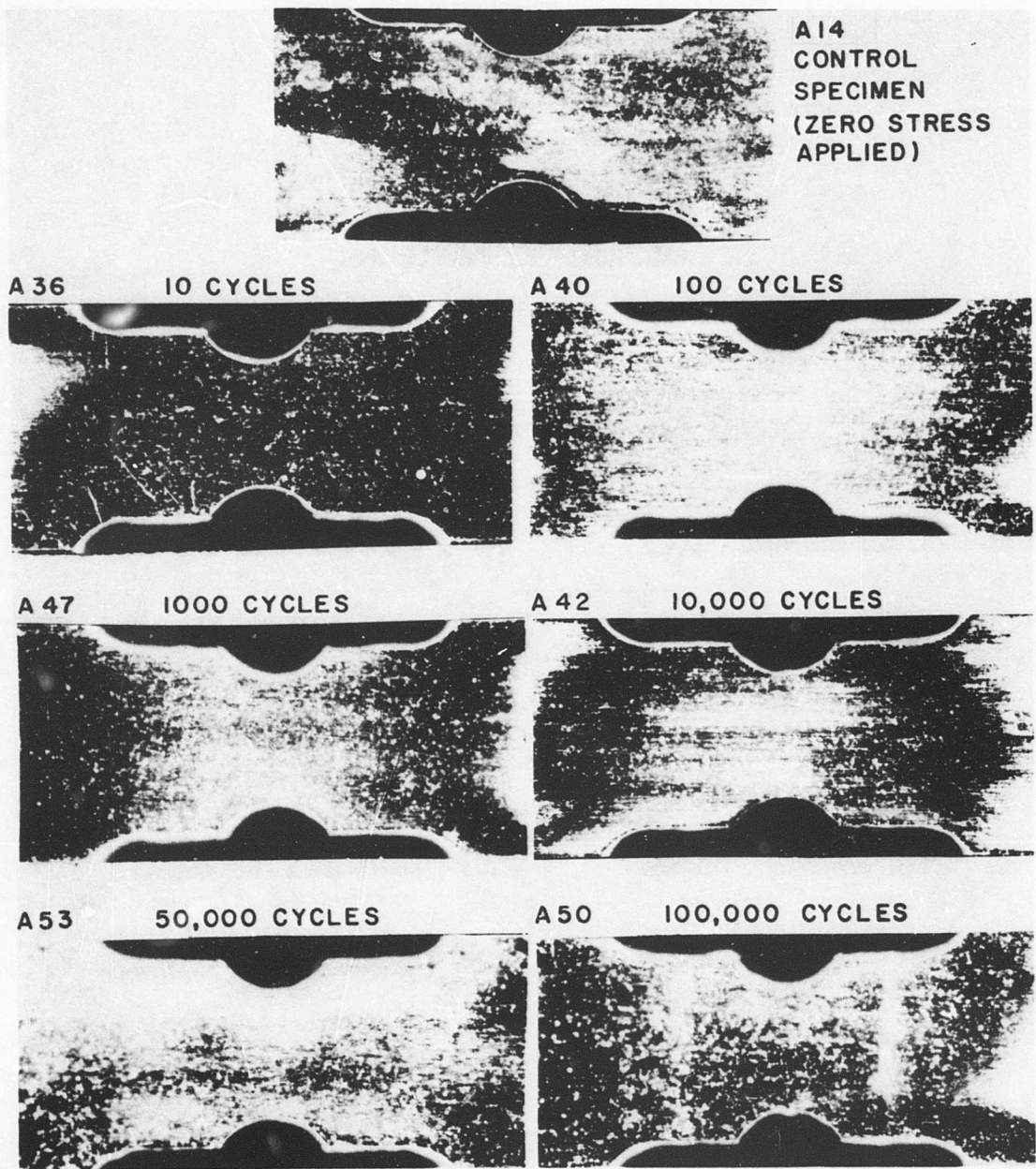


Figure 7. Autoradiographs of Fatigued 2024 Aluminum Specimens
(Max. Load, 35 Ksi).

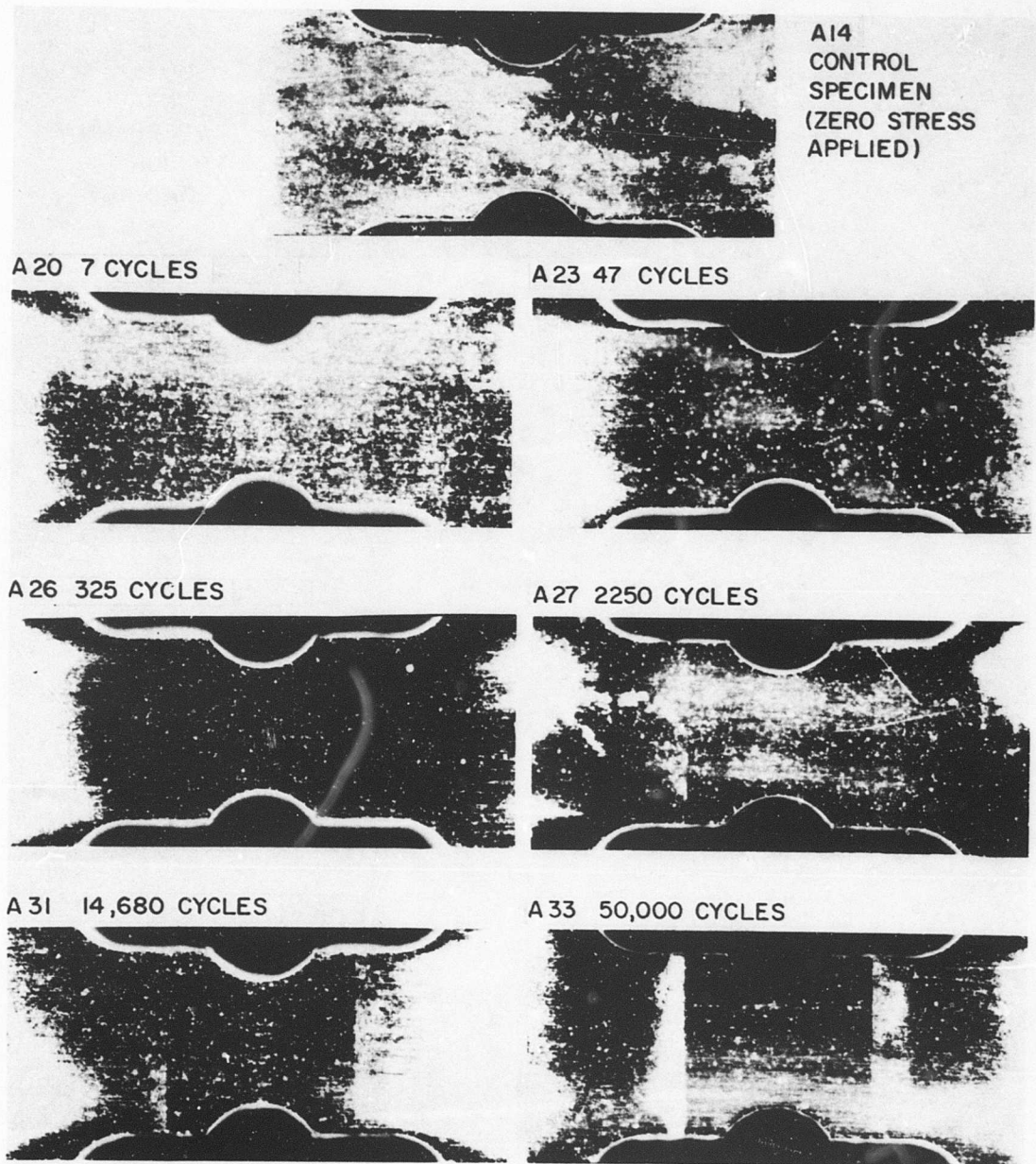


Figure 8. Autoradiographs of Fatigued 2024 Aluminum Specimens
(Max. Load, 45 Ksi).

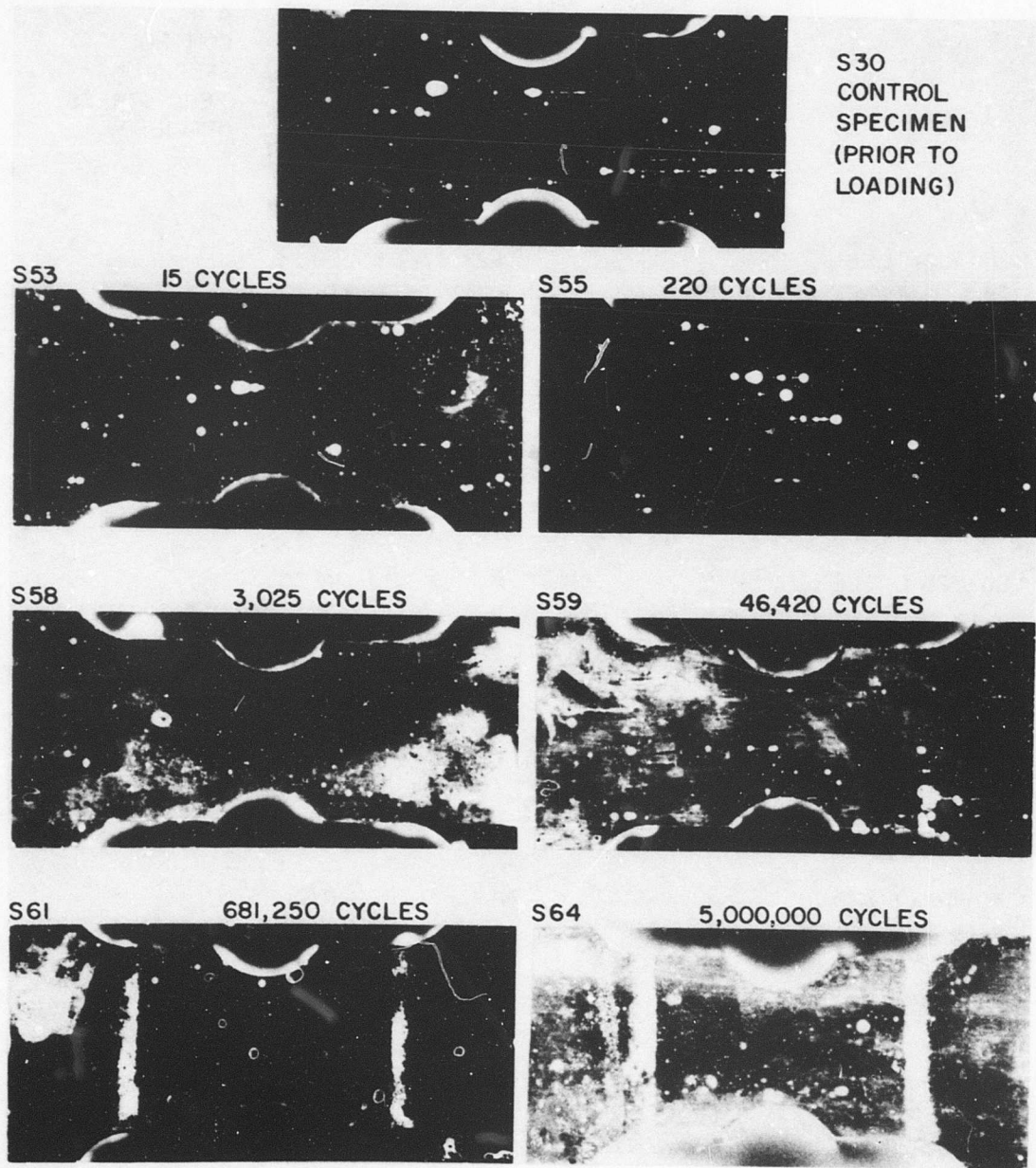


Figure 9. Autoradiographs of Fatigued 4130 Steel Specimens (Max. Load, 75 Ksi).

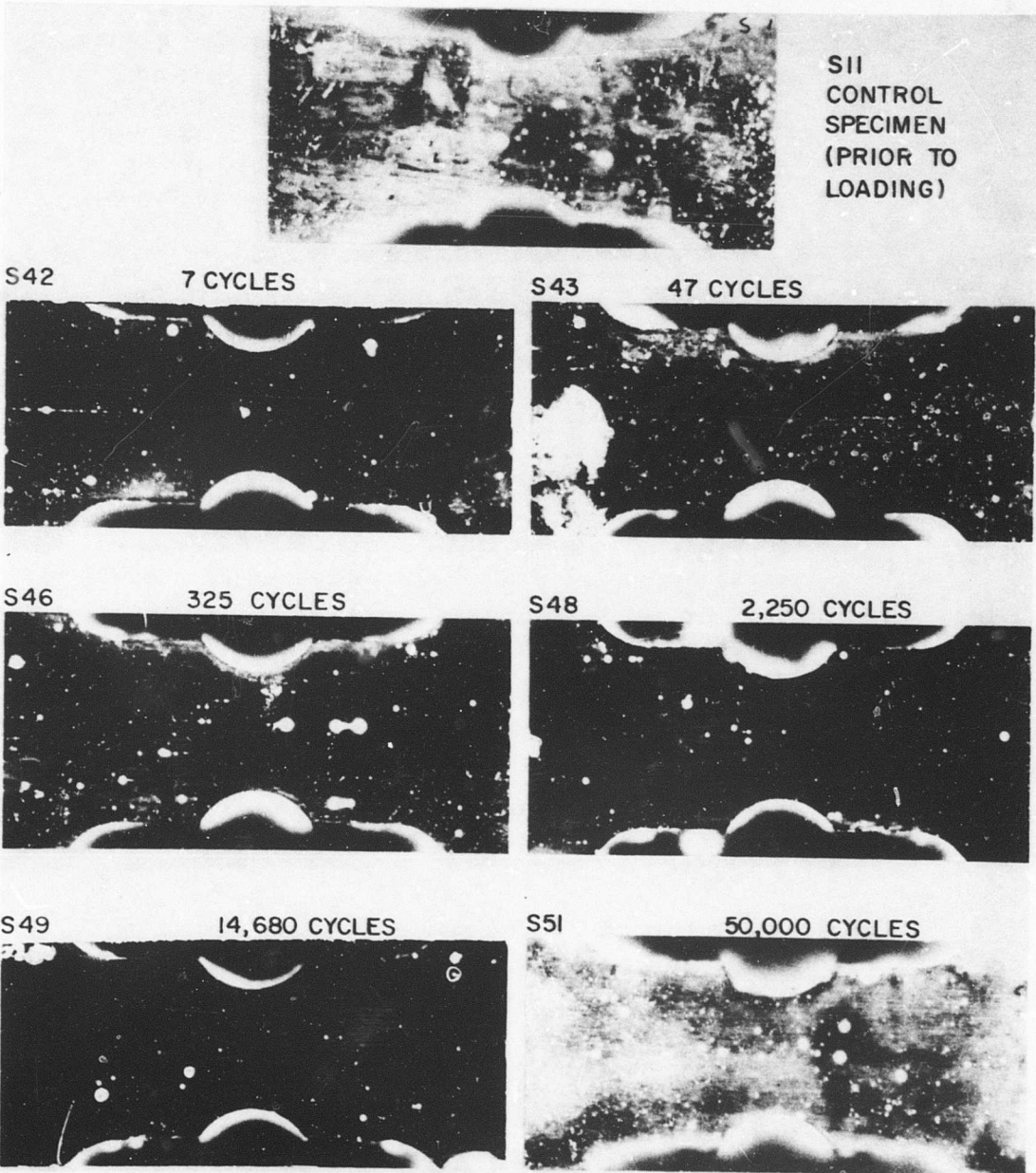


Figure 10. Autoradiographs of Fatigued 4130 Steel Specimens (Max. Load, 87.5 Ksi).

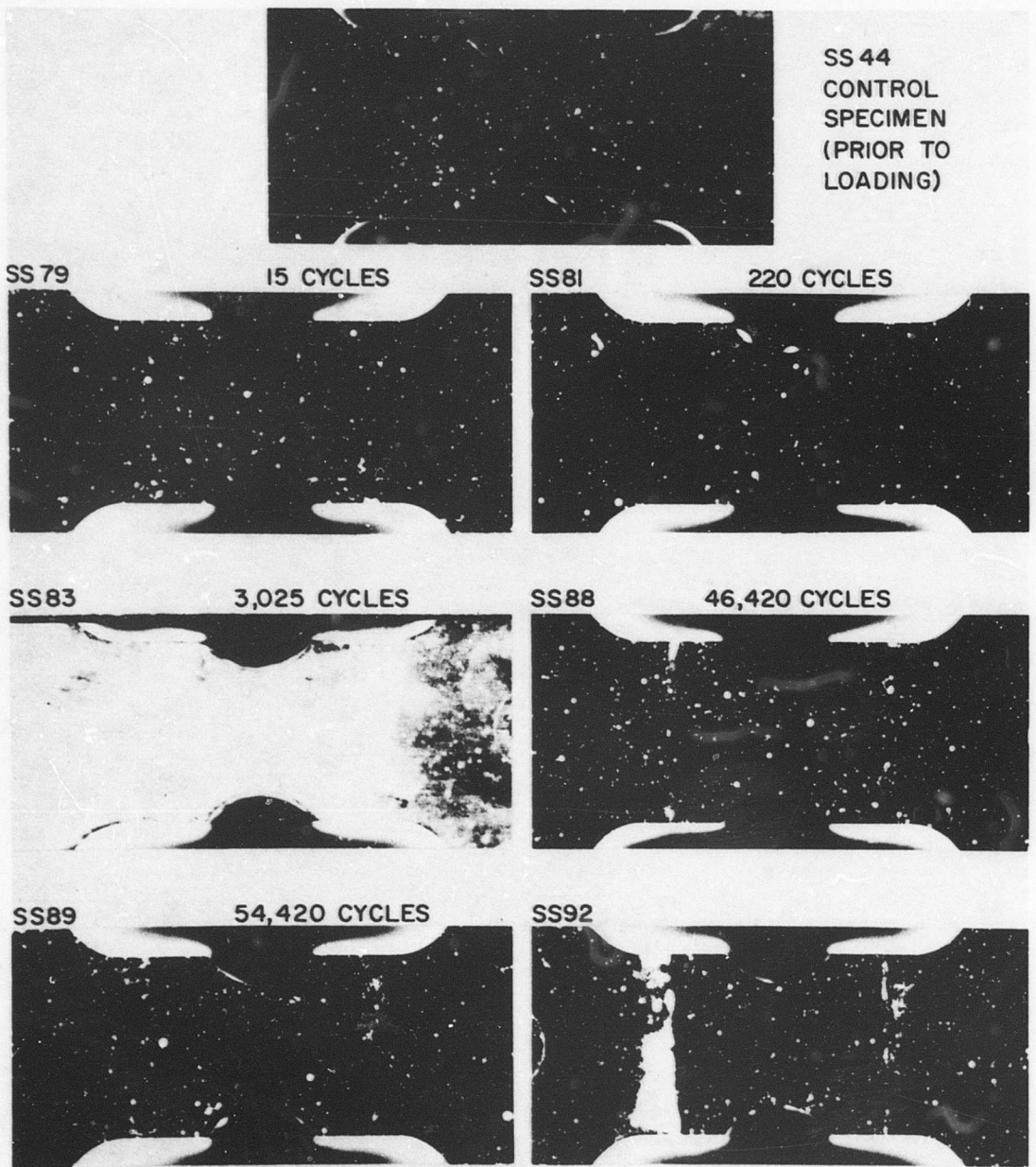


Figure 11. Autoradiographs of Fatigued 301 Stainless Steel Specimens
(Max. Load, 108 Ksi).

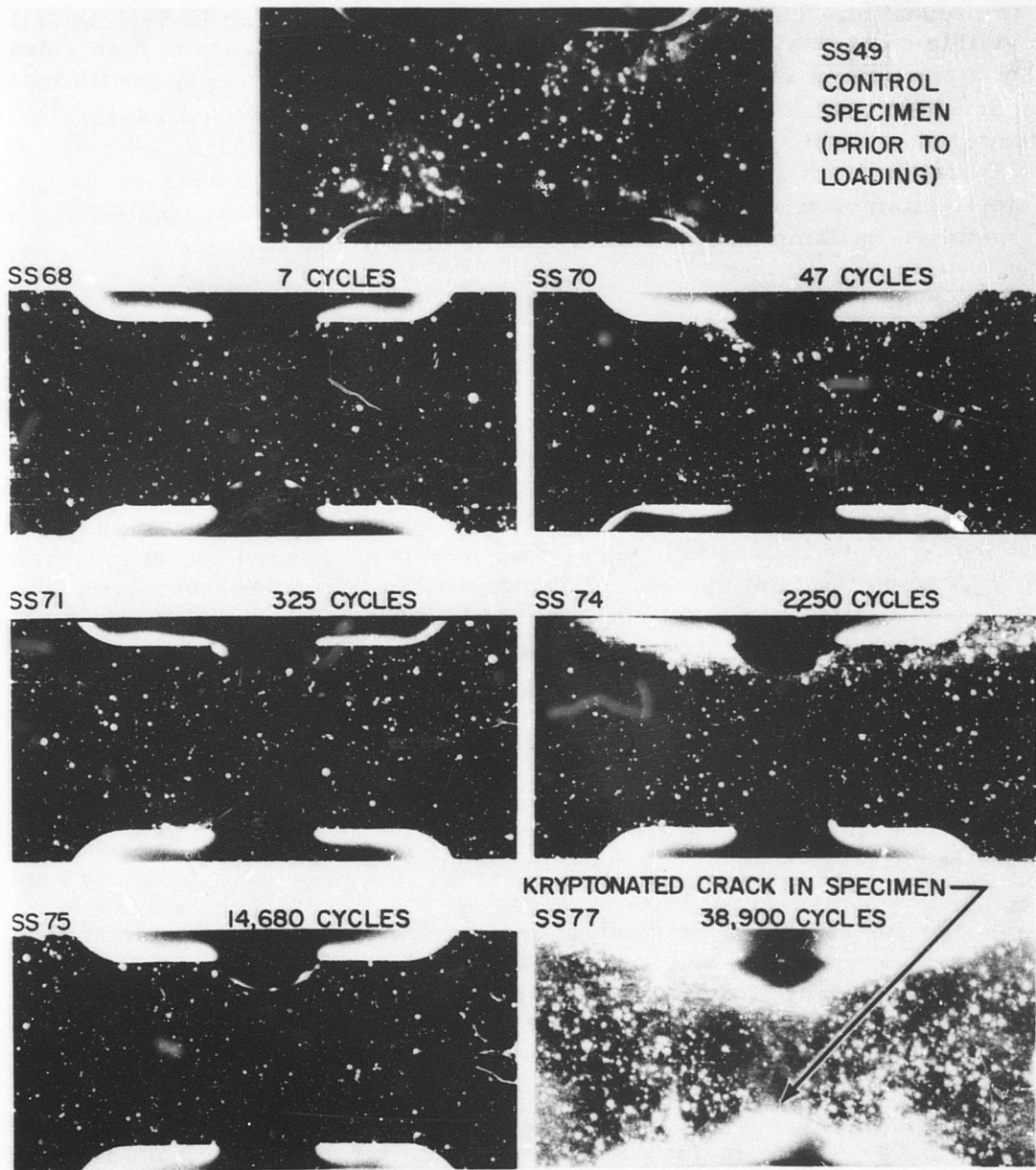


Figure 12. Autoradiographs of Fatigued 301 Stainless Steel Specimens
(Max. Load, 117.5 Ksi).

increased number of fatigue cycles. There were no unusual increases in Kr-85, even around the fractured regions present in Figures 5 and 6. However, the cracks observed in Figures 5, 6, and 12 are heavily impregnated. The cracks indicated in Figures 5, 6, and 12 are optically visible on each specimen, are indicated in autoradiographs of both sides of a specimen, and are less than 2 mils in width. However, the effort to correlate fatigue history with krypton absorption was not successful by autoradiographic means either. The wide vertical bands present in Figures 6, 7, 8, 9, and 11 outside the notched region are due to the application of stress by the fatigue machine. Tension was applied to the specimens by clamping onto either side of the notched region.

4.2 Kr-85 RELEASE

The examination of the release of Kr-85 from specimens which had been fatigued involved several aspects. Specific examination procedures were as follows:

- (1) For each stress indicated in Subsection 3.4 of this study and for each material, three kryptonated specimens were fatigue cycled and radiometrically measured at zero load prior to cycling, at maximum load on the first cycle, and at mean load at six other points in the fatigue life. Since fatigue life is a logarithmic function of stress cycles, these six other points were at logarithmic intervals in the anticipated fatigue life.
- (2) The specimens of (1) above and all specimens involved in Section 4.1, Kr-85 absorption, were heated and kept at constant temperature to outgas the Kr-85. The retention of Kr-85 with heating time was examined using the fatigue history of the specimen as a parameter.
- (3) Specimens of 4130 normalized steel and 301 half hard stainless steel were kryptonated and then fatigued to 30%, 45%, 60%, and 75% of their average life at a selected stress level. Autoradiographic comparisons of a specimen's activity distribution were made at these percentages and with the initial condition.
- (4) Specimens of 4130 normalized steel and 301 half hard stainless steel were kryptonated, fatigued to 90% of their average life, and fatigued to failure at the three stress levels indicated in Subsection 3.4 of this report. Autoradiographs were made initially, at the 90% of average life point, and at failure to examine retention changes.

The kryptonation parameters for the specimens involved in this phase of the study were a temperature of 300° F, a pressure of 125 psia, and a duration of 16 hours. The specimens involved in item (2) above had more than one set of kryptonation parameters for all specimens, since some specimens were used from the absorption testing phase of the study.

4.2.1 Fatigue Process

Twelve kryptonated specimens of each of the three metals were fatigue cycled and the specimen activity was monitored during cycling at Battelle Memorial Institute. Nine of the twelve were fatigued to specimen failure. The three metals each showed different test results and are separately discussed. The 301 half hard stainless steel curves of Kr-85 concentration in the specimen versus number of fatigue cycles are shown in Figures 13, 14, and 15. As observable in all the latter figures, the krypton concentration changed quite markedly at the first cycle of tension. This release caused as much as a 50% decrease in activity from the initial activity after only one stress cycle and indicates a sensitivity to tensile stress of Kr-85 in a 301 half hard stainless steel lattice. This property was not further examined in this study. The property of study interest, namely, the change of retained krypton with increased specimen fatigue, was positively observed with only one 301 stainless steel specimen (Figure 13). The activity decrease in Figure 13 from 10,000 cycles to failure at 270,000 cycles is about 15%. Figures 14 and 15 do not exhibit this decrease in concentration with increased fatigue.

The 4130 normalized steel did not indicate a Kr-85 loss during the testing procedure. However, after approximately a 1-week time lapse after fatiguing, the 4130 steel specimens indicated significantly reduced concentrations of Kr-85 radiometrically. The specimens were autoradiographed, and two are shown in Figures 16 and 17. The spatial detail of the loss indicates a loss of krypton in the high stress region where fracture was imminent (in Figure 16) and where fracture actually occurred (in Figure 17). Not only did the Kr-85 leave the region where cracking occurred, but the peripheral region of the crack shows krypton loss. The relation of this region to the "plastic" behavior of metals undergoing high stress fatiguing would be metallurgically of interest, but this relation was not investigated in this study. Since the 4130 steel did not immediately lose krypton in the fatiguing process and since oxidation is known to cause krypton loss from a material, the relation of the Kr-85 loss to metallurgical properties is not straightforward. The specimen in Figure 16 was cracked but still in one piece; the specimen in Figure 17 had been broken in testing.

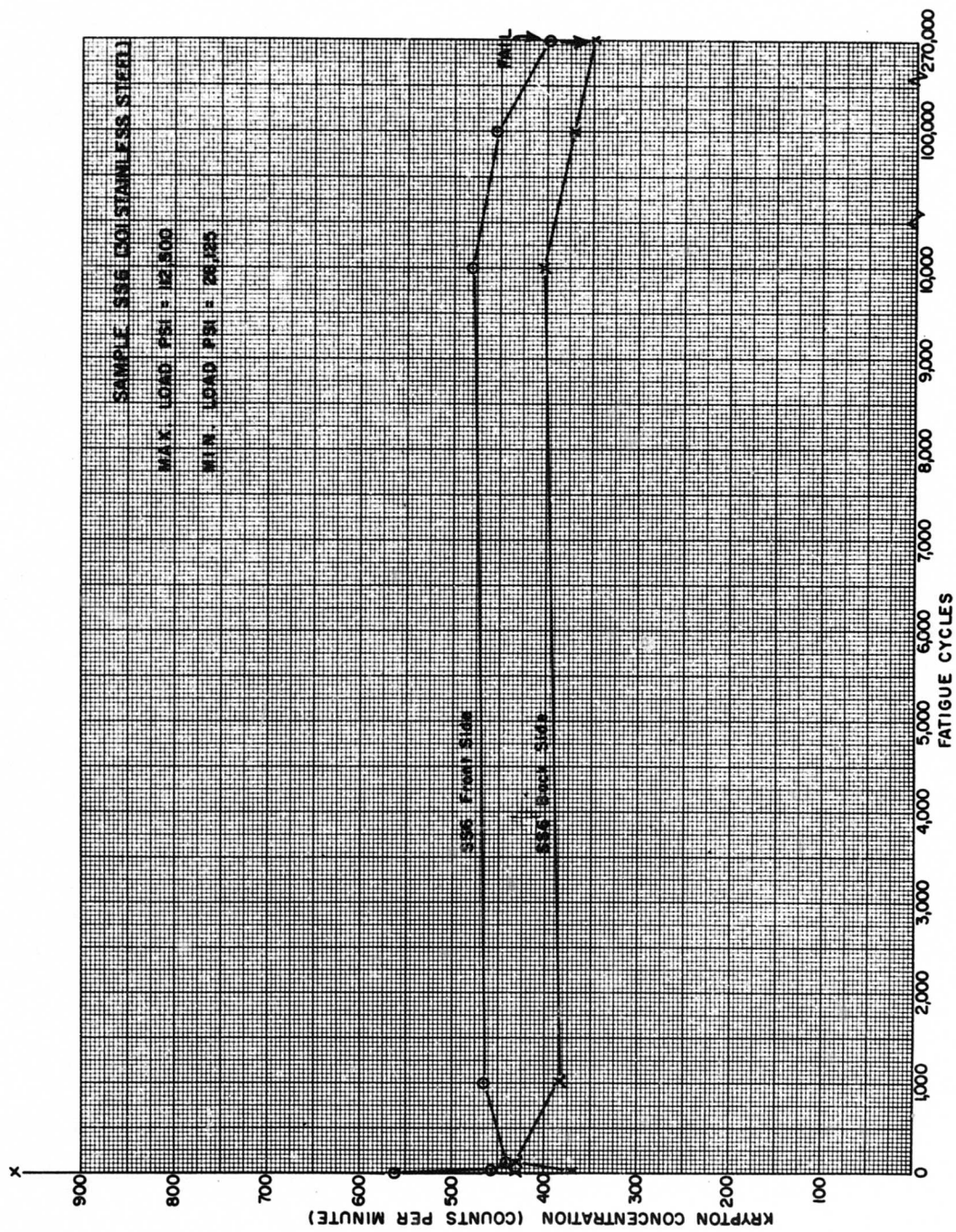


Figure 13. Activity Versus Fatigue Life for Stainless Steel Specimen.

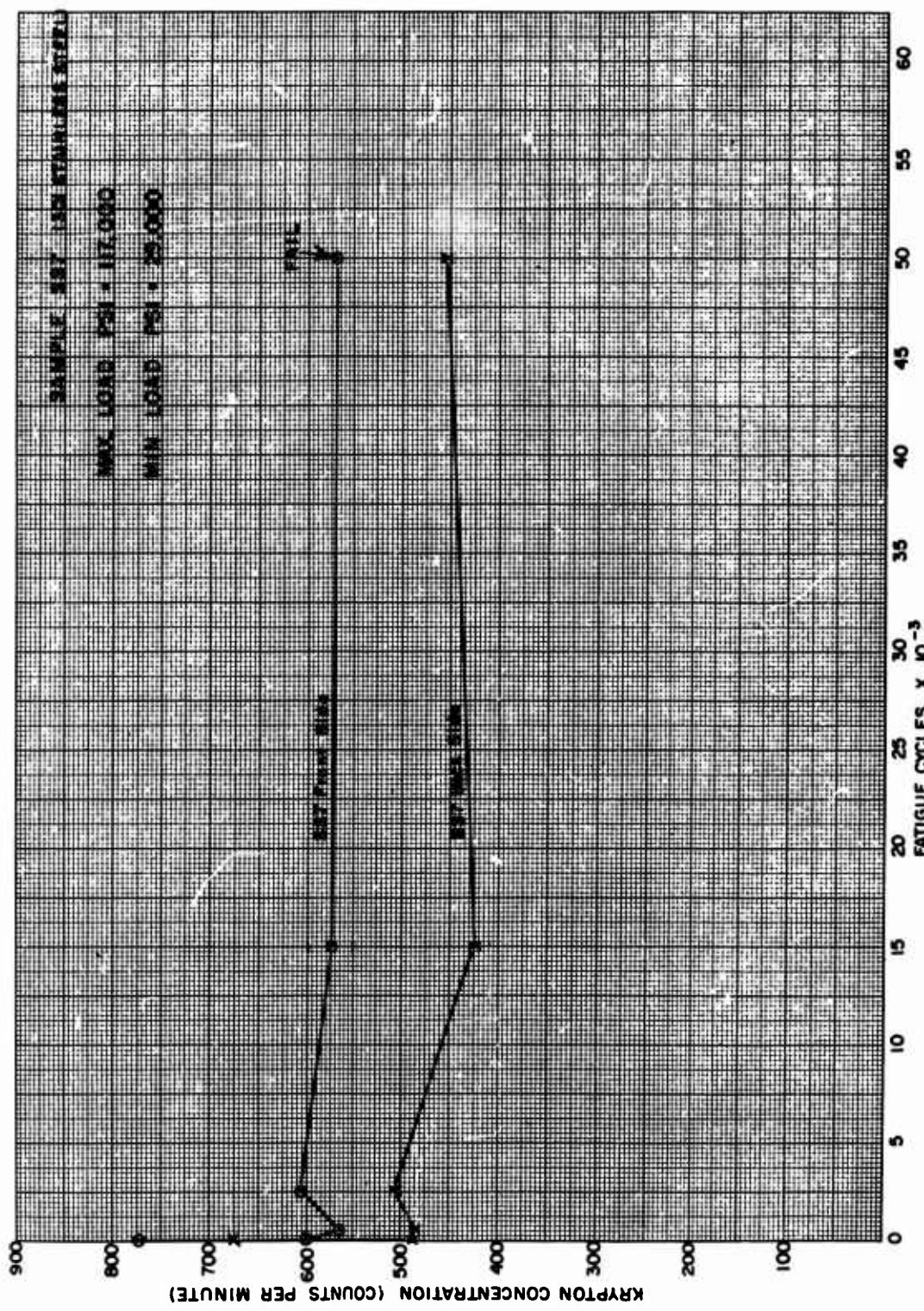


Figure 14. Activity Versus Fatigue Life for Stainless Steel Specimen.

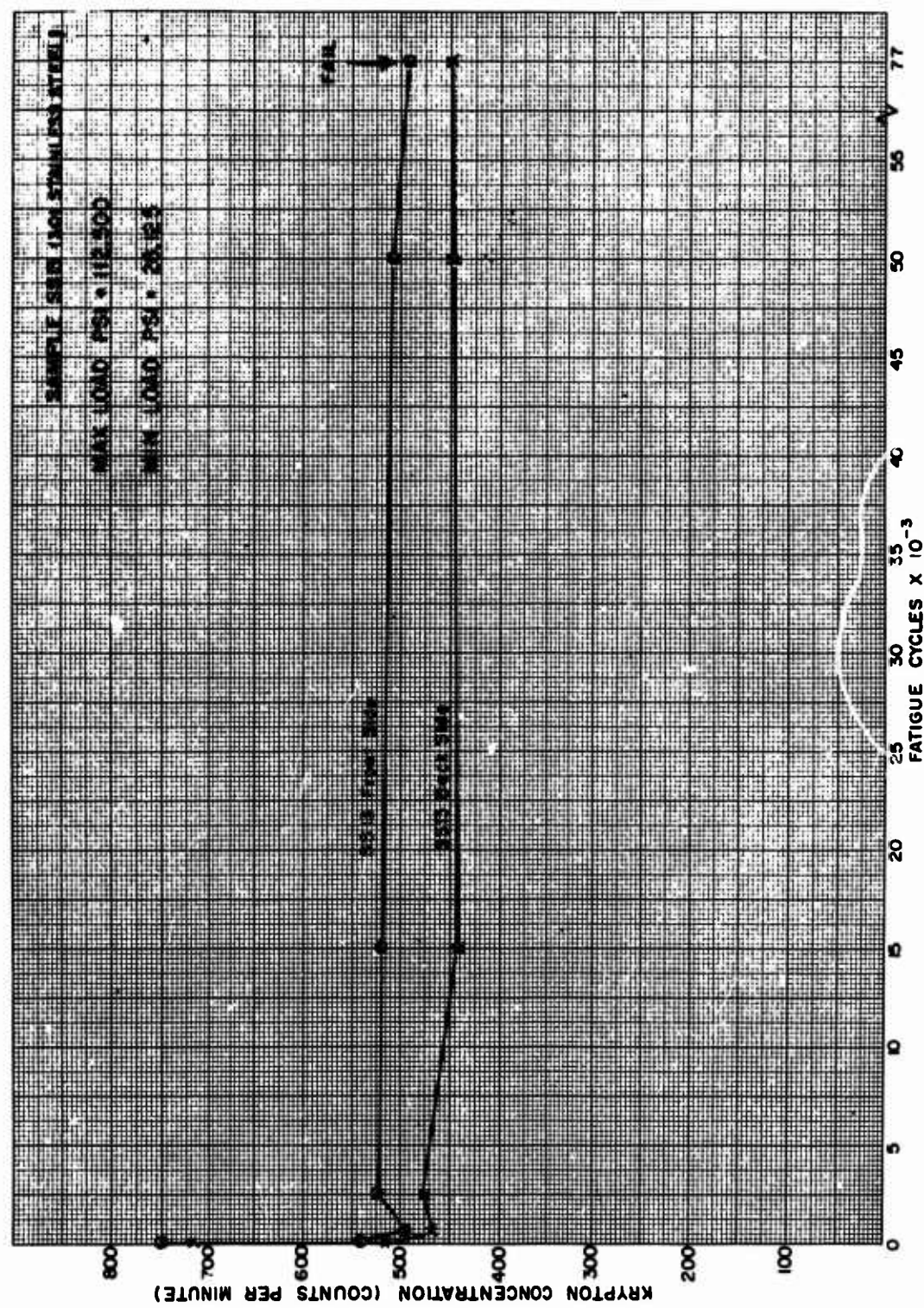
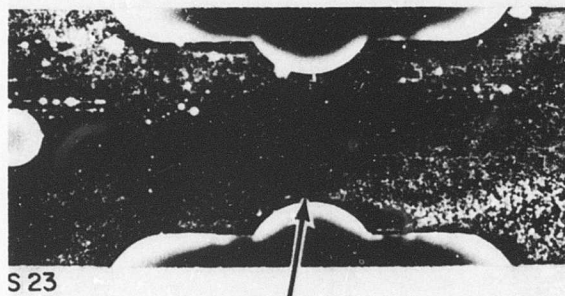


Figure 15. Activity Versus Fatigue Life for Stainless Steel Specimen.

CRACK OBSERVED AFTER 85,500 CYCLES
FRONT FACE



AREAS OF HIGH FATIGUE AND CRACKING



BACK FACE

Figure 16. Autoradiographs of Fatigued 4130 Steel Specimen.
(Max. Load, 78 Ksi).

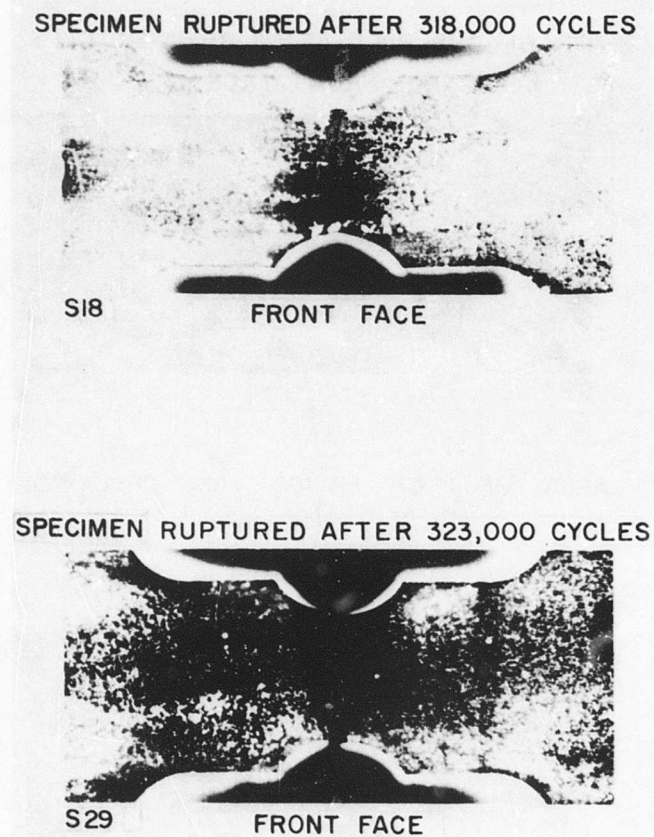


Figure 17. Autoradiographs of Fatigued 4130 Steel Specimens (Max. Load, 80 Ksi).

The 2024-T3 aluminum specimens gave no indication of response to the fatigue cycling process during or at any time after the fatiguing process. Autoradiographs taken two weeks after the fatigue cycling process for one specimen are shown in Figure 18. There is a small, optically visible crack in the specimen of Figure 18, but this was not detected in the autoradiograph. Also, there was no release in the region of the crack to indicate the beginning of fatigue cracking, which differs from the 4130 steel results. The line-like loss regions in Figure 18 were named a "wood grain" effect for obvious reasons but were not understood metallurgically with certainty. Several other specimens exhibited this effect after fatiguing. This specimen was later outgassed, rekrryptonated, and autoradiographed. The "wood grain" effect was no longer present but the crack mentioned above was definitely observable.

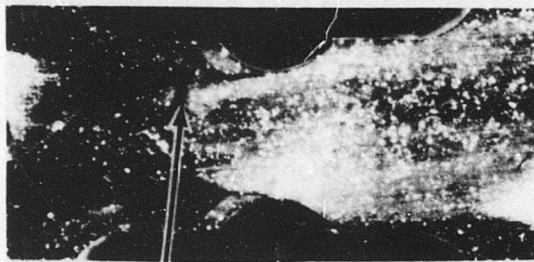
The aluminum did not release krypton related to stress fatigue history. Since aluminum tends to oxide rapidly in air, it was considered feasible that during the kryptonation process the aluminum oxide surface layer was kryptonated and not the unoxidized metal region. To examine this, two aluminum specimens were hand polished with a jeweler's cloth, and Kr-85 activity measurements were made every 10 polishing strokes. The resulting curve of Kr-85 retention versus number of strokes decreased asymptotically to a value about one-tenth the original concentration. The end point of polishing was qualitatively made when a high metallic polish was observed. The specimens were allowed to reoxidize in air for two days and remeasured for activity. No indication of activity in the specimens was found. This indicated the following:

- (1) Since roughly 90% of the Kr-85 was in the oxide, the metal was not the primary absorber of krypton.
- (2) During the process of oxidation, krypton is released from 2024-T3 aluminum.
- (3) The fatigue properties of the surface oxide layer of aluminum and not those of the aluminum metal itself were predominantly examined with Kr-85 unless there was an interaction of the metal with the oxide layer.

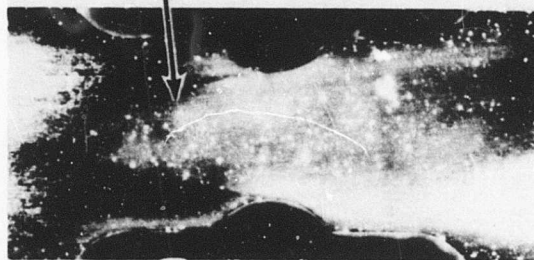
4.2.2 Retention With Time

The specimen used in Section 4.1, which had been first fatigued and later kryptonated, and the specimens used in Subsection 4.2.1, which had been first kryptonated and then fatigued, were heated and kept at constant

SPECIMEN A6
FRONT SIDE



"WOOD GRAIN" EFFECT



SPECIMEN A6
BACK SIDE

Figure 18. Autoradiographs of Fatigued 2024 Aluminum Specimens.

temperature for a total period of 3 hours. Radiometric measurements were made on the specimens each 0.5 hour. The correlation of Kr-85 retention in fatigued specimens with time as compared to the retention in unfatigued specimens with time was of interest. The data from samples which had been first kryptonated and later fatigued will be considered first.

Figure 19 indicates the results obtained when 2024-T3 aluminum specimens were exposed to a temperature of 300°F for a duration of 3 hours. The right side of Figure 19 shows the average control curve composed of data from four unfatigued specimens, and the left side indicates that differences between separate fatigued specimens were not sufficient to justify individual curves except for specimen A7. The control curve data showed at least a $\pm 5\%$ dispersion about an average curve at each retention measurement interval. The data pertinent to the specimens fatigued to failure are shown on the left side of Figure 19. Specimen A7 is a singular example of a change in Kr-85 retention with fatigue history, since for all other fatigued specimens the average curves of the fatigued and unfatigued specimens are very much alike. No consistent correlation was observed from these measurements between the fatigue history and Kr-85 release in 2024-T3 aluminum using a temperature of 300°F and a 3-hour heating time. The anomaly associated with specimen A7 was not further investigated.

Figure 20 illustrates the results obtained when fatigued and unfatigued 4130 normalized steel specimens were exposed to 300°F for 3 hours. As can be seen, the unfatigued specimens and the specimens fatigued to failure gave similar results. The data dispersion for both the control and fatigued curves is much greater than that found in Figure 19 for aluminum. In this case, the percent variation between front and back surfaces of the same specimen varied by as much as $\pm 15\%$, with counting statistics accounting for $\pm 6\%$ of this variation at a 2σ confidence level. The data variance at a particular exposure time is sufficient to cause an apparent increase in the average retention curves after a 3-hour heating time. Also, specimens S9 and S16 in Figure 20, which were fatigue cycled to 10^7 cycles, did not behave in a manner similar to sample A7 in Figure 19, which was fatigued to 10^7 cycles. Then no correlation was observed between Kr-85 retention and the fatigue history of 4130 normalized steel by means of these measurements.

The results of the same type of measurements on 301 half hard stainless steel are shown in Figure 21. As was observed with the 4130 steel data in Figure 20, the data dispersion for a particular exposure time is quite large. The control specimens gave a broader dispersion of data than the

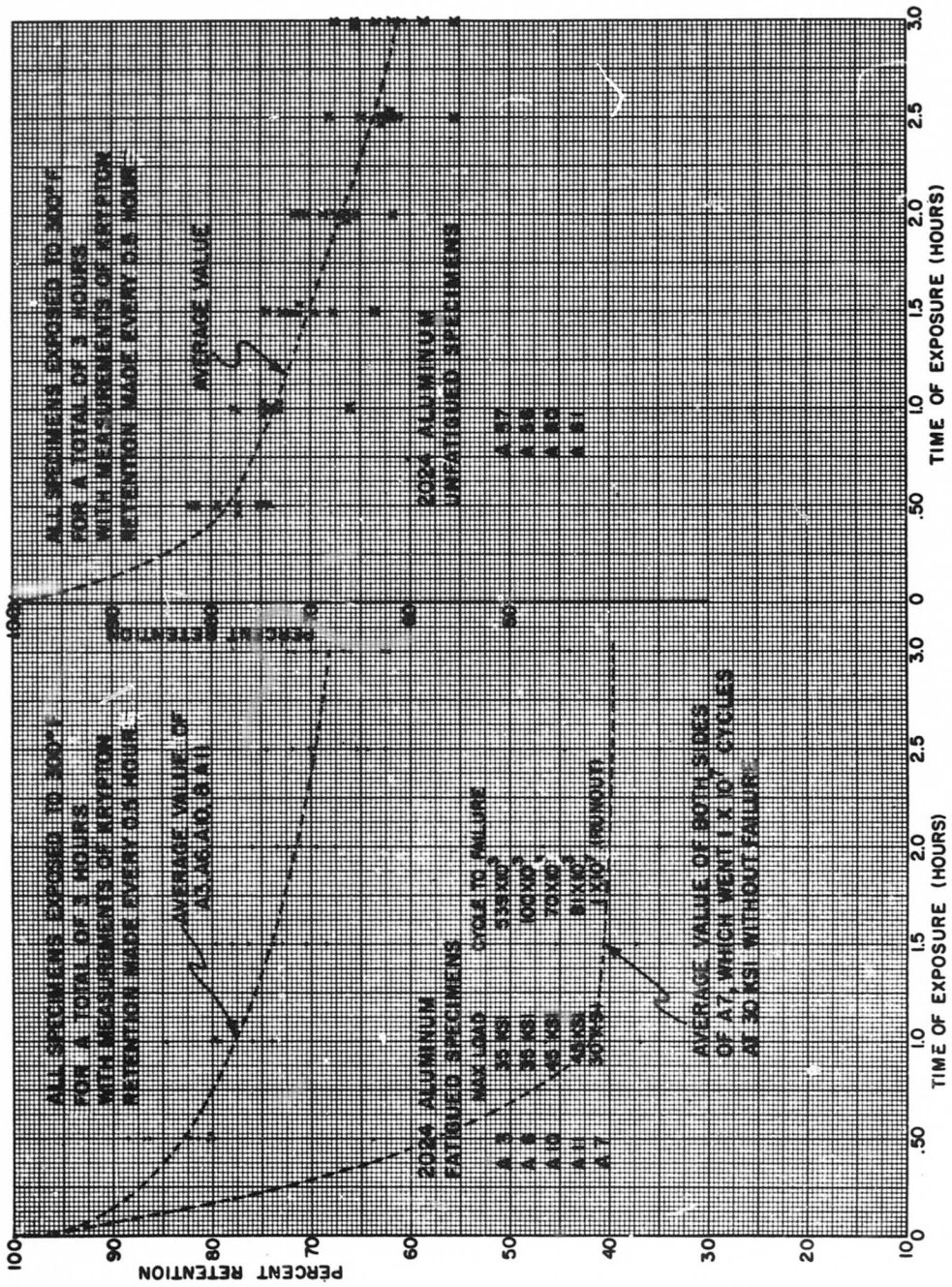


Figure 19. Outgassing Curves of 2024 Aluminum Specimens.

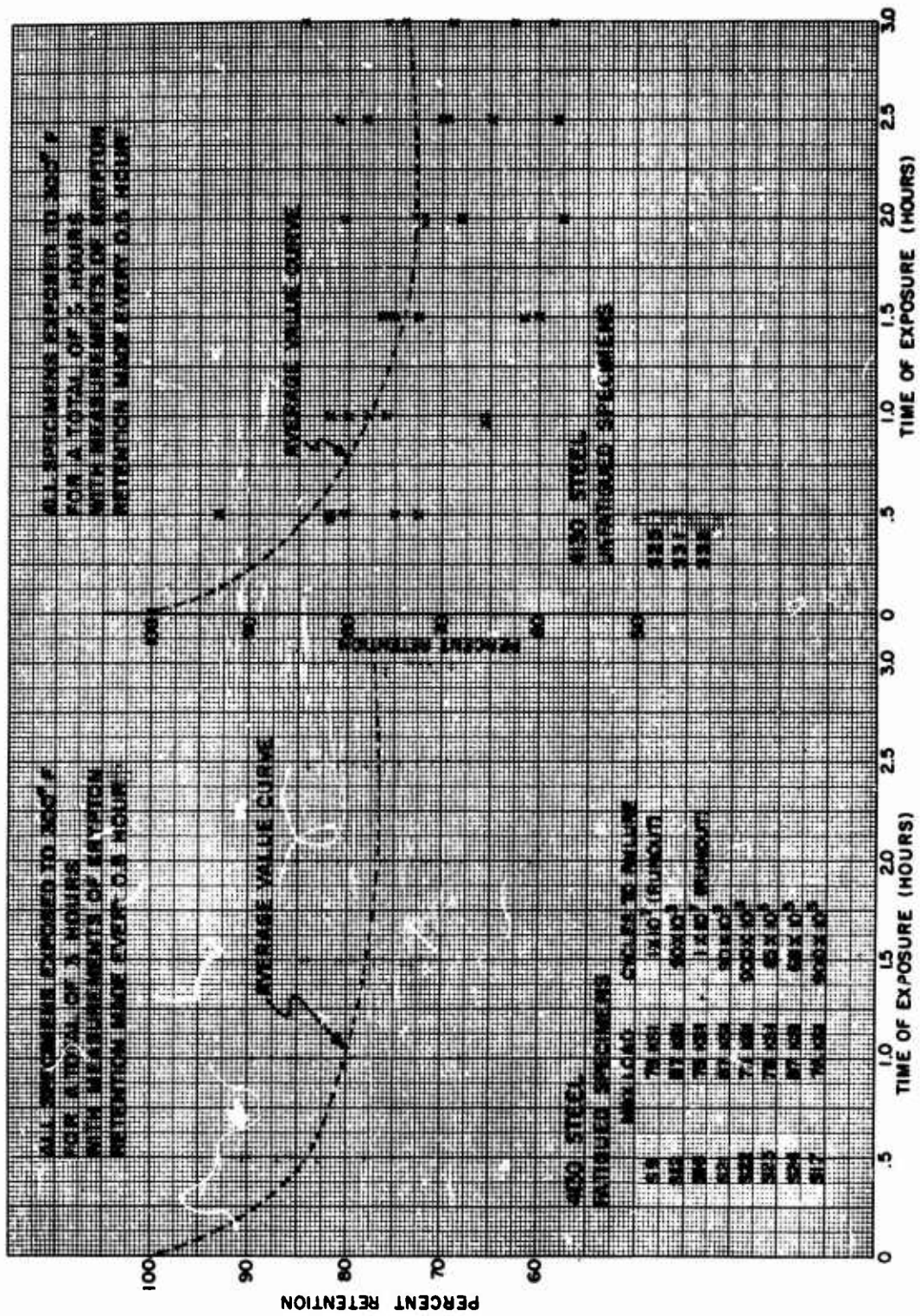


Figure 20. Outgassing Curves of 4130 Steel Specimens.

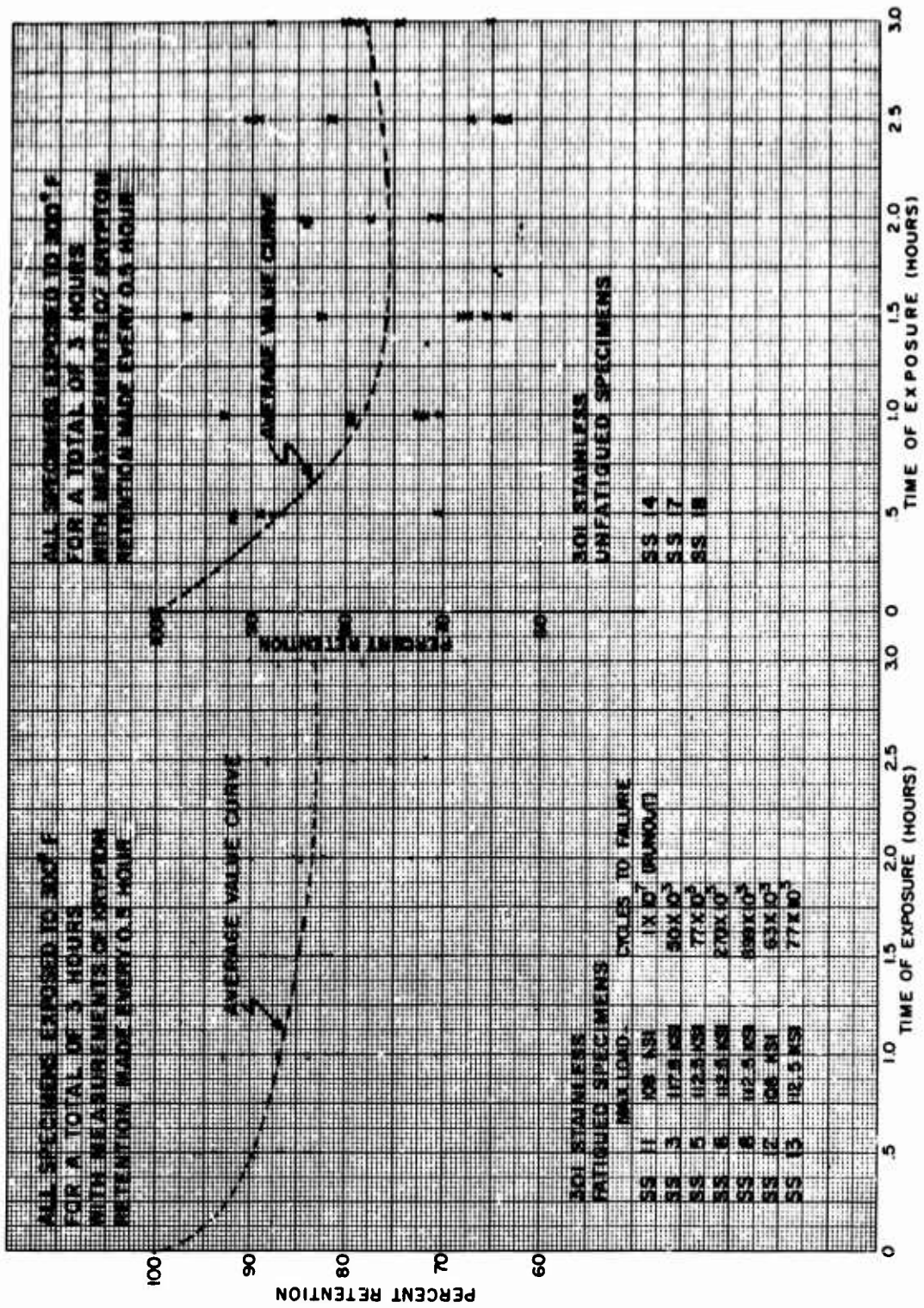


Figure 21. Outgassing Curves of 301 Stainless Steel Specimens.

fatigued specimens and indicate a less realistic retention with time control curve than Figure 20. The reason for the large data dispersion of the control curve is not known. These data do not indicate an observable correlation between fatigue history and Kr-85 retention in 301 half hard stainless steel.

The specimens involved in the absorption testing, Section 4.1 of this report, were also outgassed as a function of time, with retention measurements made each 0.5 hour. Since the specimens of Subsection 4.2.1 did not indicate a consistent correlation when outgassed at 300°F, the 2024 aluminum specimens from the absorption testing were outgassed at 400°F and the 4130 steel and 301 stainless steel specimens from the absorption testing were outgassed at 600°F. The outgassing duration of 3 hours was kept the same for these tests.

For the 54 aluminum specimens fatigued in this section of the study, the following breakdown of maximum stress level and range of fatigue cycle sampling exists:

<u>Specimens</u>	<u>Maximum Stress (Ksi)</u>	<u>Range of Fatigue Life</u>	
		<u>Samples</u>	<u>Cycles</u>
A68 - A85	30	15	5×10^6
A36 - A53	35	10	5×10^5
A18 - A35	45	7	5×10^4

The specimens were grouped for outgassing according to the maximum stress level used in the fatigue cycling. The results of heating to 400°F for 3 hours are shown in Figures 22, 23, and 24. The fatigued specimens indicate a greater data dispersion about a curve formed from average values of retention at a particular exposure time, but the control curve and average value curve are quite similar. In Tables IX, X, and XI the percent retention of Kr-85 as a function of heating time, with the number of fatigue cycles as a parameter, is given for the three stress levels used. From these data, it may be observed that grouping of the data with the same fatigue history to form curves of retention versus time does not give more meaningful results than the average curve formed from all data. There was no correlation found between fatigue history and krypton retention with time for 2024-T3 aluminum when the specimens were heated and measured in the manner described.

The results of the same test procedure applied to 4130 normalized steel and 301 half hard stainless steel are shown in Tables XII through XV and Figures 25 through 28. Both the tabulated results and the figures indicate that the variation in data at a specific exposure time is too great to evaluate any correlation between Kr-85 retention and fatigue history for

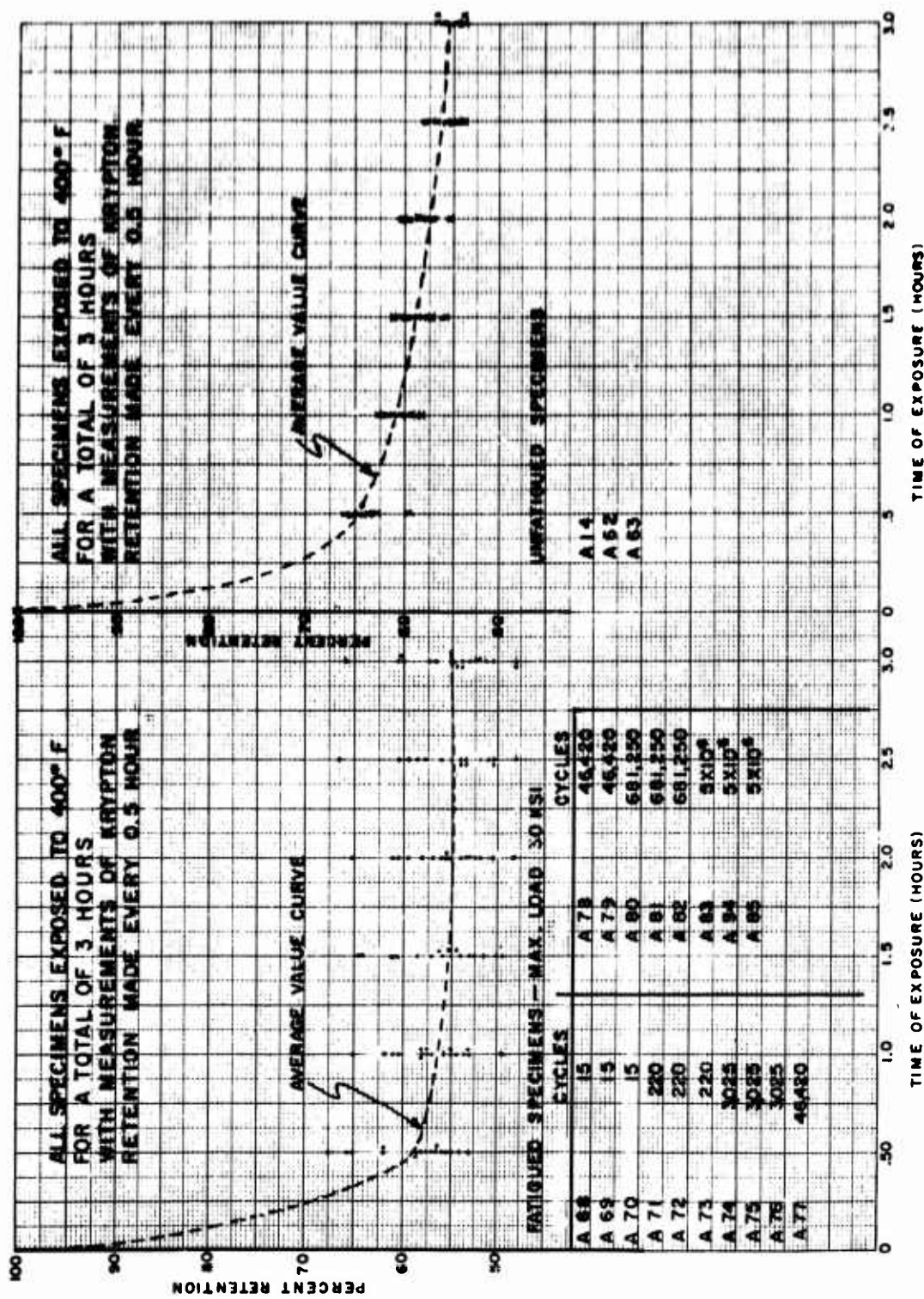


Figure 22. Outgassing Curves of 2024 Aluminum Specimens.

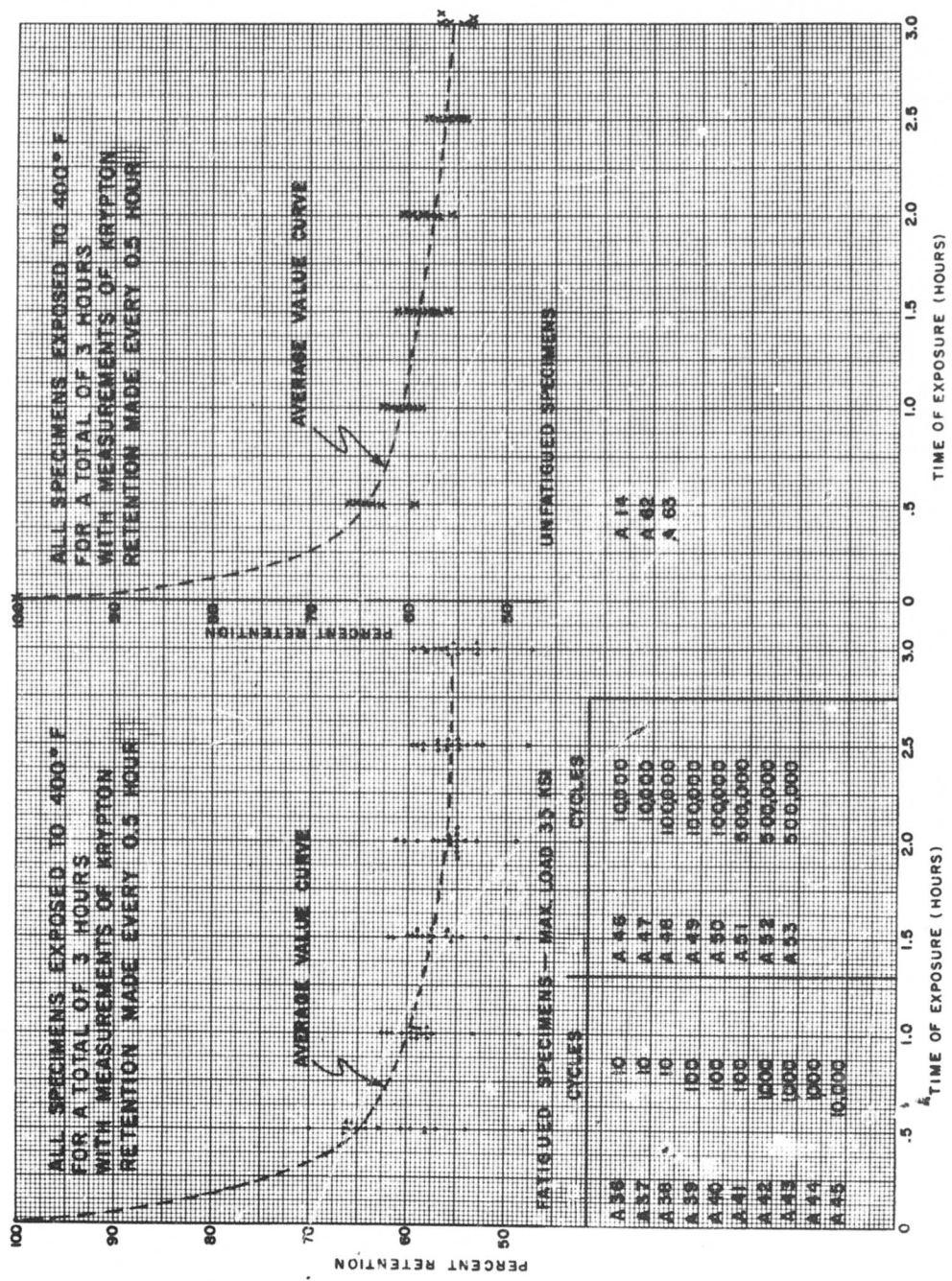


Figure 23. Outgassing Curves of 2024 Aluminum Specimens.

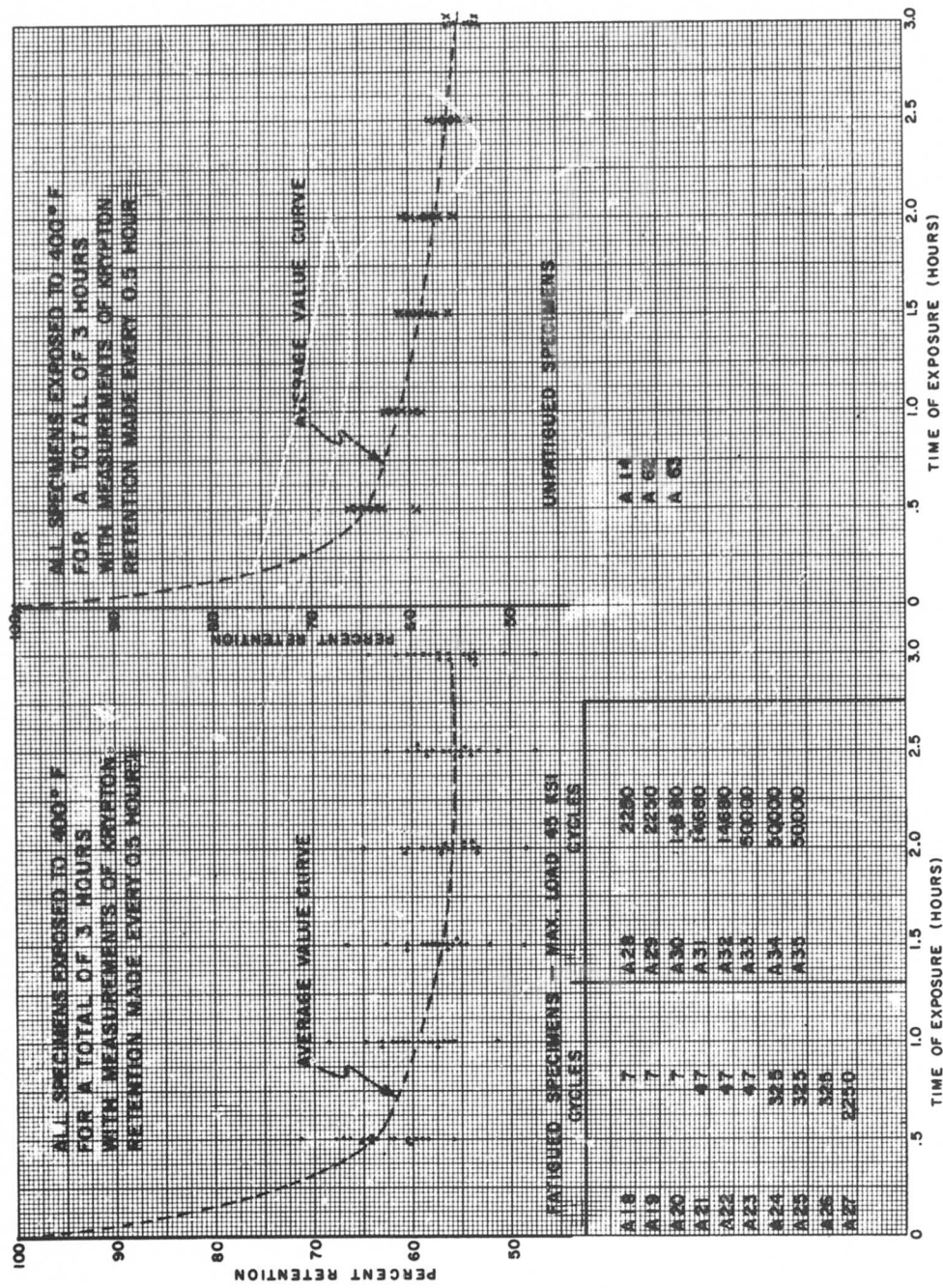


Figure 24. Outgassing Curves of 2024 Aluminum Specimens.

TABLE IX. 2024-T3 ALUMINUM RETENTION
DATA (MAX. LOAD, 30 KSI)

Specimen Number	Percent Retention After:						Cycles
	0.5h	1.0h	1.5h	2.0h	2.5h	3.0h	
A68	56.0	53.0	56.0	52.5	51.1	52.5	15
A69	54.2	53.5	54.2	53.3	52.0	52.1	15
A70	55.4	55.0	52.8	54.0	54.2	53.7	15
A71	57.4	56.2	57.3	58.2	58.8	57.1	220
A72	65.0	62.6	64.5	60.5	60.6	60.7	220
A73	62.1	61.1	60.8	61.1	59.2	59.9	220
A74	55.5	55.0	55.0	55.7	53.5	55.0	3,025
A75	67.5	65.2	54.3	65.3	66.4	65.4	3,025
A76	61.8	60.3	61.0	59.6	58.4	60.2	3,025
A77	58.2	57.6	56.2	56.1	55.9	56.8	46,420
A78	56.5	55.8	54.6	55.2	54.9	53.8	46,420
A79	56.3	57.6	53.0	53.0	53.6	51.3	46,420
A80	58.8	58.2	58.5	57.2	58.0	54.0	681,250
A81	53.2	53.3	51.4	50.4	50.3	50.5	681,250
A82	58.8	57.9	49.9	51.9	50.4	48.7	681,250
A83	66.5	54.6	54.9	55.6	54.3	54.3	5,000,000
A84	57.3	49.5	49.5	48.3	48.2	48.5	5,000,000
A85	59.0	46.7	49.1	46.1	47.1	45.3	5,000,000
A14 (control)	63.0	58.7	56.0	55.6	55.0	54.0	0
A62 (control)	64.5	62.3	59.3	58.0	55.8	56.5	0
A63 (control)	63.7	61.7	57.8	58.4	56.0	54.0	0

TABLE X. 2024-T3 ALUMINUM RETENTION
DATA (MAX. LOAD, 35 Kips)

Specimen Number	Percent Retention After:						
	0. 5h	1. 0h	1. 5h	2. 0h	2. 5h	3. 0h	Cycles
A36	59. 6	59. 6	61. 4	61. 3	59. 5	58. 4	10
A37	65. 1	58. 8	59. 0	56. 9	56. 9	58. 3	10
A38	62. 7	57. 8	57. 8	56. 0	54. 7	56. 4	10
A39	70. 0	61. 6	59. 1	55. 8	59. 3	59. 4	100
A40	60. 5	62. 5	61. 7	60. 3	58. 8	57. 7	100
A41	66. 3	61. 8	56. 2	55. 5	55. 1	53. 3	100
A42	56. 8	59. 0	58. 5	59. 0	55. 5	53. 0	1,000
A43	66. 2	57. 9	55. 6	54. 3	54. 1	54. 5	1,000
A44	64. 2	57. 7	57. 4	55. 0	53. 2	53. 0	1,000
A45	66. 1	60. 6	60. 0	56. 5	58. 5	56. 8	10,000
A46	64. 4	59. 0	56. 0	54. 9	54. 9	55. 3	10,000
A47	57. 0	58. 0	55. 5	55. 8	56. 0	51. 3	10,000
A48	65. 6	59. 3	59. 6	57. 3	56. 9	56. 1	100,000
A49	66. 0	59. 3	57. 4	55. 1	56. 1	55. 4	100,000
A50	58. 0	57. 7	54. 5	55. 0	56. 0	55. 0	100,000
A51	54. 1	53. 2	52. 0	53. 2	52. 5	53. 2	500,000
A52	49. 2	48. 6	48. 5	48. 8	47. 7	47. 2	500,000
A53	58. 0	58. 5	57. 8	55. 0	57. 2	54. 0	500,000
A14 (control)	63. 0	58. 7	56. 0	55. 6	55. 0	54. 0	0
A62 (control)	64. 5	62. 3	59. 3	58. 0	55. 8	56. 5	0
A63 (control)	63. 7	61. 7	57. 8	58. 4	56. 0	54. 0	0

TABLE XI. 2024-T3 ALUMINUM RETENTION
DATA (MAX. LOAD, 45 Kips)

Specimen Number	Percent Retention After:						
	0.5h	1.0h	1.5h	2.0h	2.5h	3.0h	Cycles
A18	65.0	61.8	58.2	58.7	58.6	58.8	7
A19	66.8	63.3	62.6	60.8	60.5	61.5	7
A20	64.2	64.7	60.6	60.6	59.4	60.2	7
A21	60.4	57.7	56.4	56.4	55.3	56.2	47
A22	62.0	60.6	58.8	57.3	56.8	57.3	47
A23	64.0	63.2	57.8	61.0	58.0	58.0	47
A24	58.5	55.8	54.6	53.5	51.3	50.4	325
A25	60.3	58.8	57.4	56.7	56.2	56.1	325
A26	67.0	59.3	60.5	59.2	59.6	59.6	325
A27	71.5	68.3	66.7	65.0	62.5	64.2	2,250
A28	60.4	58.9	52.3	53.6	53.2	53.4	2,250
A29	59.2	58.3	56.0	54.8	55.0	54.0	2,250
A30	59.7	56.0	55.2	53.9	54.1	54.1	14,680
A31	64.5	61.3	59.0	57.2	58.7	57.2	14,680
A32	60.2	57.5	56.8	54.8	55.6	54.5	14,680
A33	62.4	62.0	56.5	57.5	54.0	53.5	50,000
A34	55.8	51.4	48.7	49.5	47.2	47.2	50,000
A35	65.3	57.3	55.5	54.0	54.8	53.8	50,000
A14 (control)	63.0	58.7	56.0	55.6	55.0	54.0	0
A62 (control)	64.5	62.3	59.3	58.0	55.8	56.5	0
A63 (control)	63.7	61.7	57.8	58.4	56.0	54.0	0

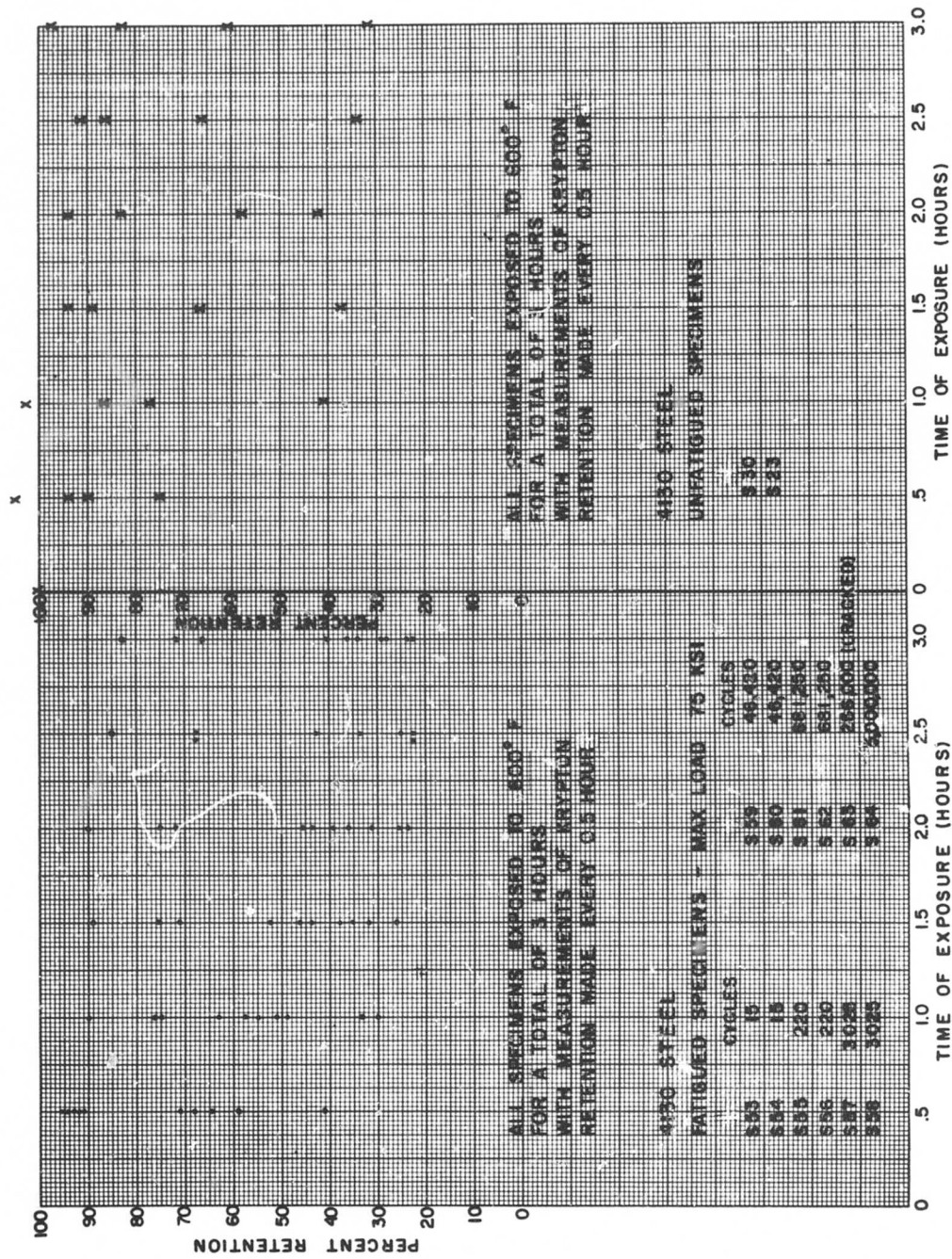


Figure 25. Outgassing Curves of 4130 Steel Specimens.

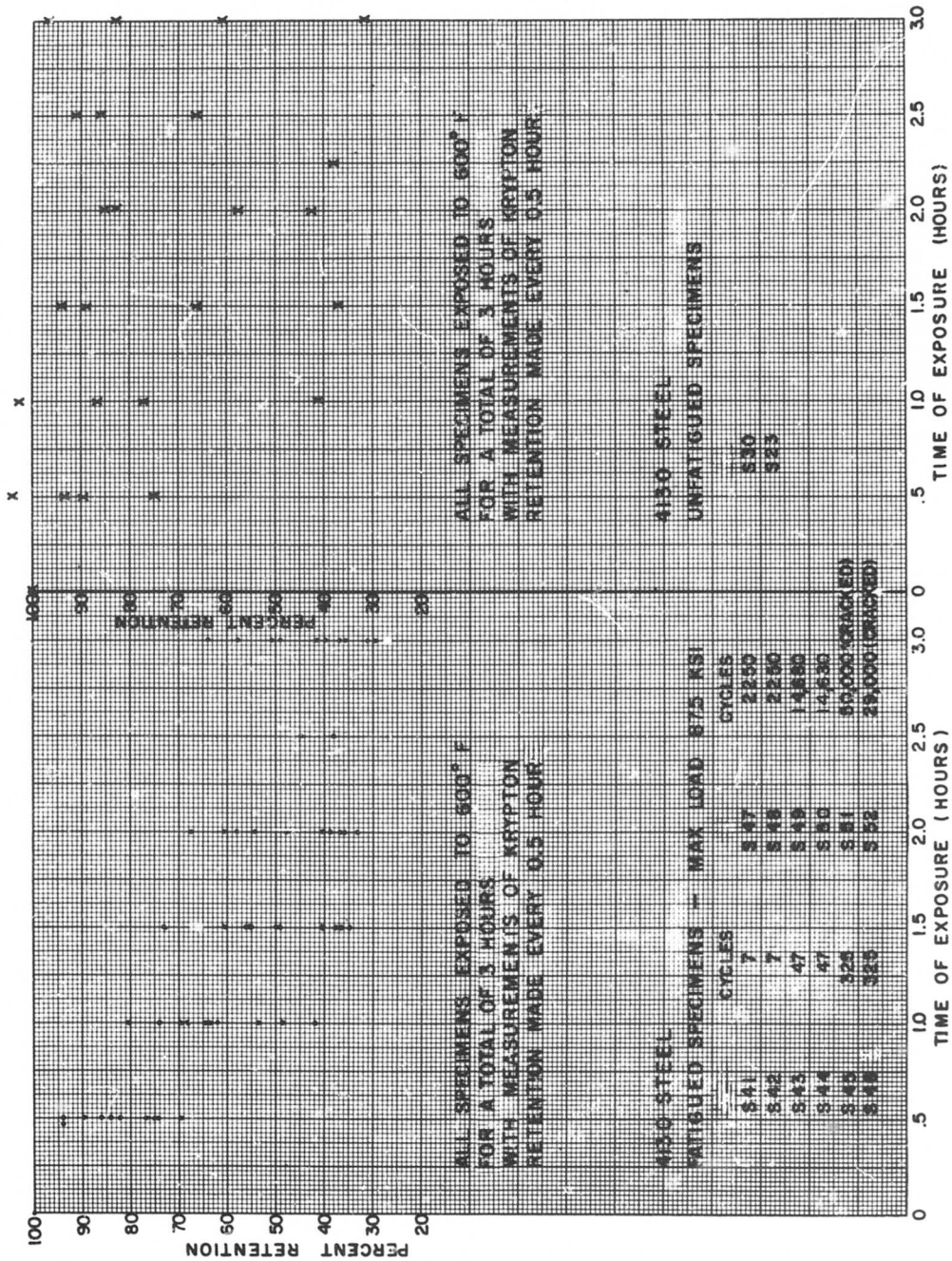


Figure 26. Outgassing Curves of 4130 Steel Specimens.

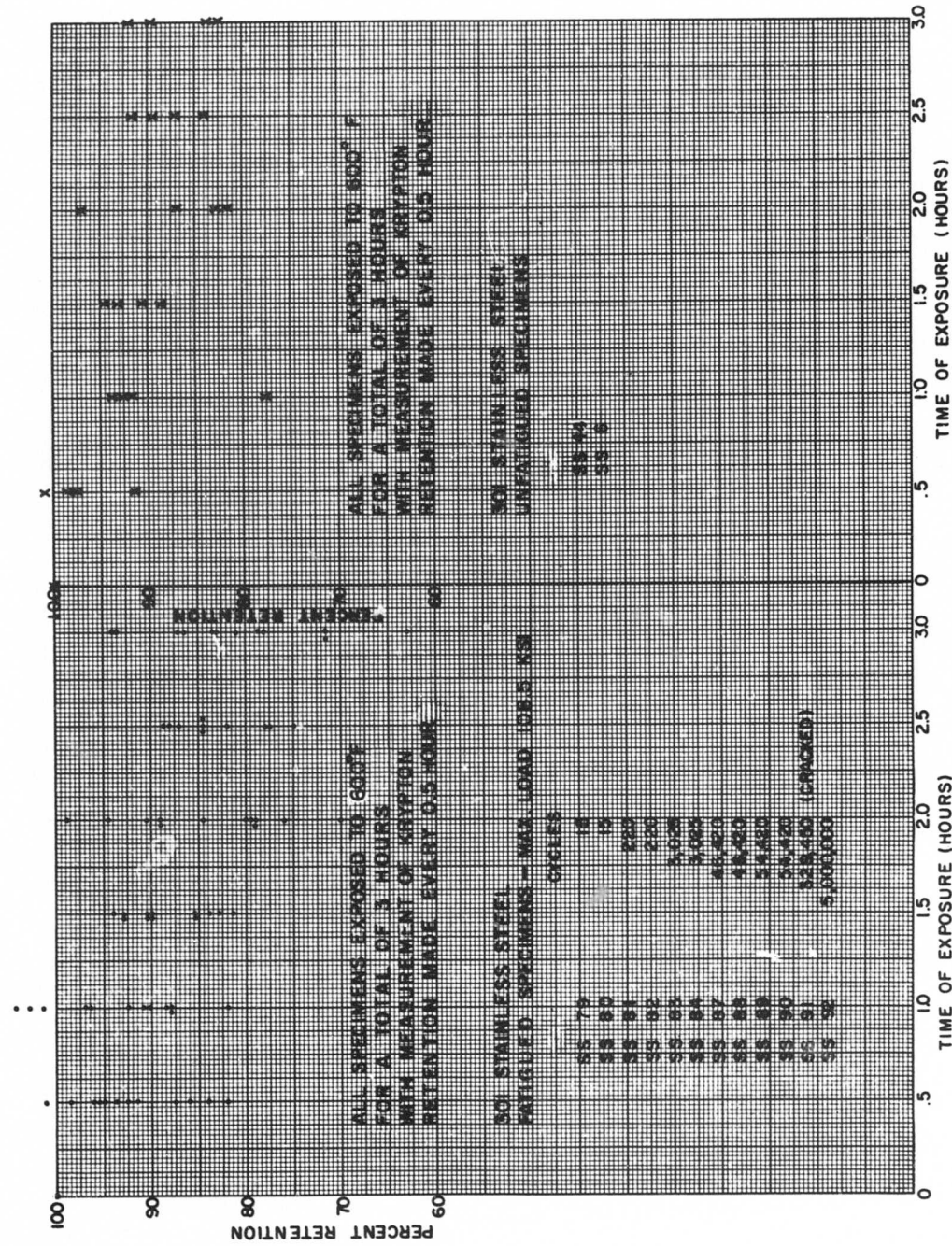


Figure 27. Outgassing Curves of 301 Stainless Steel Specimens.

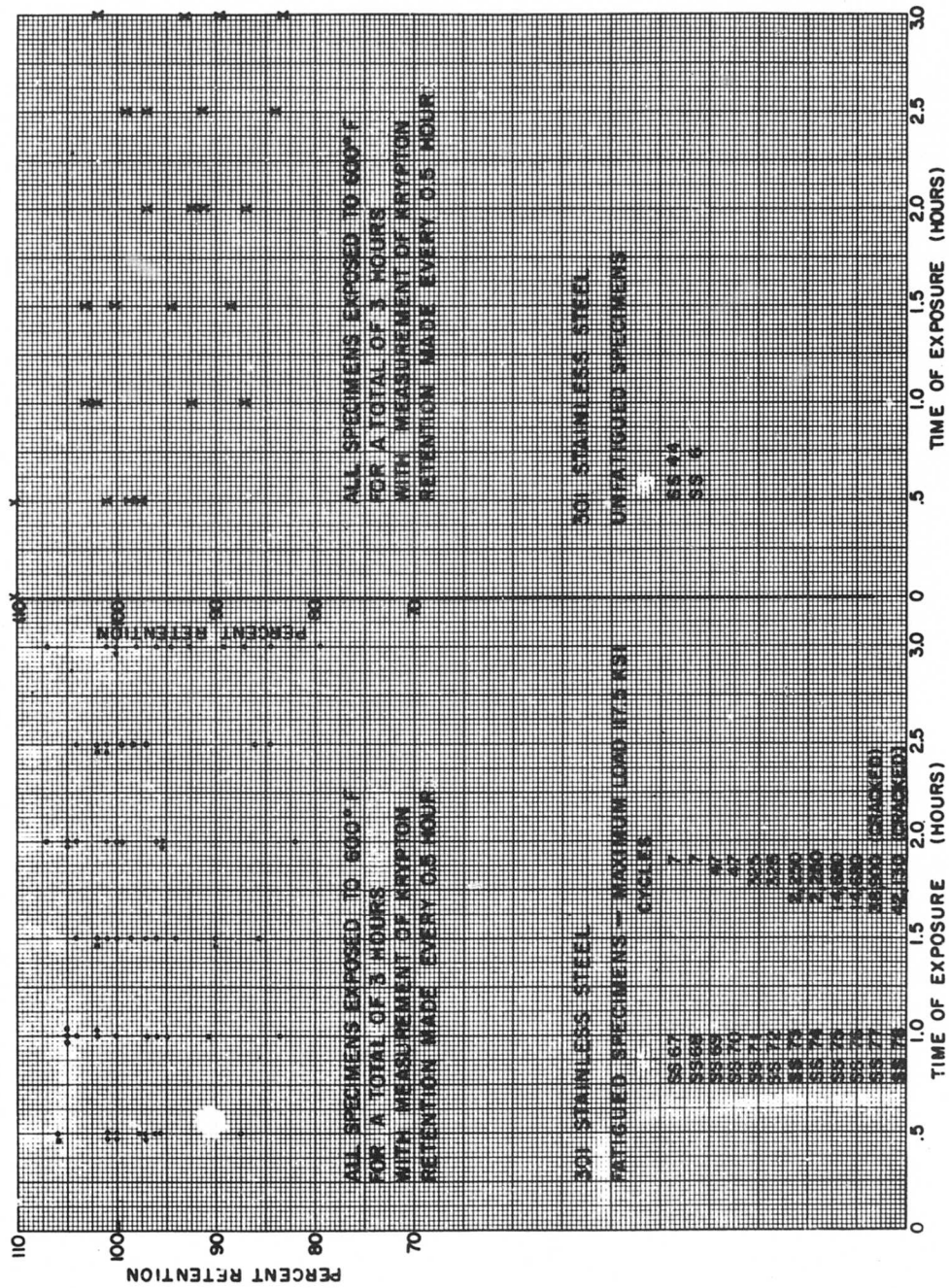


Figure 28. Outgassing Curves of 301 Stainless Steel Specimens.

TABLE XII. 4130 STEEL RETENTION
DATA (MAX. LOAD, 75 KSI)

Specimen No.	Percent Retention After:						Cycles
	0. 5h	1. 0h	1. 5h	2. 0h	2. 5h	3. 0h	
S53	64.2	63.0	52.2	45.7	42.7	40.6	15
S54	98.0	51.0	46.0	39.1	33.3	36.0	15
S55	95.2	90.4	89.1	89.9	85.0	83.0	220
S56	94.8	76.2	71.2	74.9	67.7	71.5	220
S57	71.0	48.9	31.9	31.0	22.5	22.5	3,025
S58	59.0	30.0	26.2	23.8	22.4	29.2	3,025
S59	41.0	33.3	38.2	25.7	25.0	23.3	46,420
S60	92.3	75.6	75.4	71.7	67.6	66.1	46,420
S61	65.1	44.2	46.6	43.4	37.4	36.1	681,250
S62	47.9	47.9	38.5	40.8	38.3	39.7	681,250
S63	91.6	54.4	35.3	35.9	30.8	28.3	256,000 (cracked)
S64	92.7	57.7	43.5	43.8	36.2	33.9	5,000,000

TABLE XIII. 4130 STEEL RETENTION DATA
(MAX. LOAD, 87.5 KSI)

Specimen No.	Percent Retention After:						
	0.5h	1.0h	1.5h	2.0h	2.5h	3.0h	Cycles
S41	76.5	68.0	55.0	54.1	-	48.8	7
S42	69.3	48.6	40.7	40.1	-	36.8	7
S43	75.0	53.7	37.6	33.4	-	31.0	47
S44	94.0	63.4	37.0	36.5	-	29.4	47
S45	84.3	64.1	49.2	38.8	-	35.4	325
S46	93.9	80.3	60.7	60.5	-	63.3	325
S47	85.8	74.0	73.0	67.8	-	50.3	2,250
S48	74.5	62.6	56.7	58.1	-	57.2	2,250
S49	59.0	43.4	35.6	38.0	32.9	38.0	14,680
S50	55.5	52.8	64.8	59.2	52.8	57.4	14,680
S51	82.2	41.8	34.9	35.9	37.9	41.2	50,000
S52	89.7	69.7	49.7	47.8	44.7	39.4	29,400 (cracked)

TABLE XIV. 301 STAINLESS STEEL RETENTION DATA
(MAX. LOAD, 75 Ksi)

Specimen No.	Percent Retention After:						Cycles
	0. 5h	1. 0h	1. 5h	2. 0h	2. 5h	3. 0h	
SS79	98.4	96.5	90.0	94.5	-	94	15
SS80	86.0	88.2	81.5	80.0	-	71.3	15
SS81	102	91.0	90.5	84.5	88	83.8	220
SS82	95.1	88.2	90	79.3	88.5	86.6	220
SS83	93.7	97.1	90.8	89.0	84.2	78.0	3,025
SS84	92.4	90.3	94.1	89.0	82.2	82.9	3,025
SS87	84.0	92.6	82.9	79.2	75.0	63.1	46,420
SS88	96.1	104	93.1	98.8	84.5	93.6	46,420
SS89	82.0	82.0	85.3	79.6	77.6	81.0	54,420
SS90	87.7	88.3	88.5	70.0	77.8	71.5	54,420
SS91	96.5	106	93.0	76.0	83.4	78.5	329,450
SS92	95.6	102	84.2	90.3	87.0	86.9	5,000,000

TABLE XV. 301 STAINLESS STEEL RETENTION DATA
(MAX. LOAD, 117.5 KSI)

Specimen No.	Percent Retention After:						Cycles
	0.5h	1.0h	1.5h	2.0h	2.5h	3.0h	
SS67	101	102	102	107	111	107	7
SS68	97.2	105	104	104	101	101	7
SS69	87.4	83.5	85.6	105	98.4	96.0	47
SS70	101	102	100	95.5	99.4	94.7	47
SS71	100	110	101	99.5	101	98.0	325
SS72	106	95.0	98.5	105	102	100	325
SS73	100	97.0	94.0	101	97	89.3	2,250
SS74	97.3	90.8	90.0	95.5	84.4	84.6	2,250
SS75	95.6	109	97.1	118	104	100	14,680
SS76	95.9	96.0	96.1	100	102	92.8	14,680
SS77	97.7	100	90.1	81.9	86.0	79.4	38,900 (cracked)
SS78	106	105	102	95.7	-	87	42,130 (cracked)

both 4130 steel and 301 stainless steel. The control data are noticeable in their large dispersion at a particular exposure time, with statistical uncertainty accounting for less than $\pm 8\%$, at a 2σ confidence level, of the up to $\pm 30\%$ variation from an average datum at a specific exposure time. The reason for the wide data dispersion of control specimens is not known. Since the fatigue sample data also showed large data dispersion, it was not significant to indicate retention versus time curves using the number of fatigue cycles as a parameter. Clearly, no significant variations were exhibited between fatigued and unfatigued specimens from these results.

4.2.3 Retention Over Useful Cycle Life

An examination of the integral behavior of the stress fatigued region of specimens was made in Subsection 4.2.1 by radiometric means. To examine the high stress area (the notched specimen region) with high spatial resolution, autoradiographs were made of eight 4130 steel and eight 301 stainless steel samples which had been fatigued to 30%, 45%, 60% and 75% of their average fatigue life at a chosen stress level. The specimens involved had been first kryptonated and then fatigued. Figures 29 and 30 indicate the results of this procedure. The specimens were autoradiographed both before and after fatigue cycling, but no changes were observed in the high stress regions of these autoradiographs either. Figures 29 and 30 show that no correlation is observed in the fatigue history and the krypton retention for 4130 steel and 301 stainless steel at the stress levels used. Figure 30 does indicate a loss of krypton from cracks in the metal at the notched region. This is comparable to the increase in Kr-85 concentration noted when samples were fatigued until cracked and then kryptonated (Figures 5, 6, and 12).

4.2.4 Retention Near Failure

Two specimens of both 4130 normalized steel and 301 half hard stainless steel were stress fatigued to 90% and 100% of average fatigue life after having first been kryptonated. Due to testing machine difficulties and unusual specimens, none of the specimens were fatigued to failure as planned. Autoradiographs were made of the specimens before fatiguing, at 90% of average life, and at 100% of average life or when the specimens were inappropriately broken. Figures 31 through 34 indicate results of this testing. No loss regions are observed in the high stress regions, but this may be due to testing failures encountered. For example, two specimens failed at the bolt hole; one failed at the grip; and one survived well beyond the predicted average fatigue life. However, the specimens of Figures 16 and 17 of Subsection 4.2.1, which were broken or near separation,

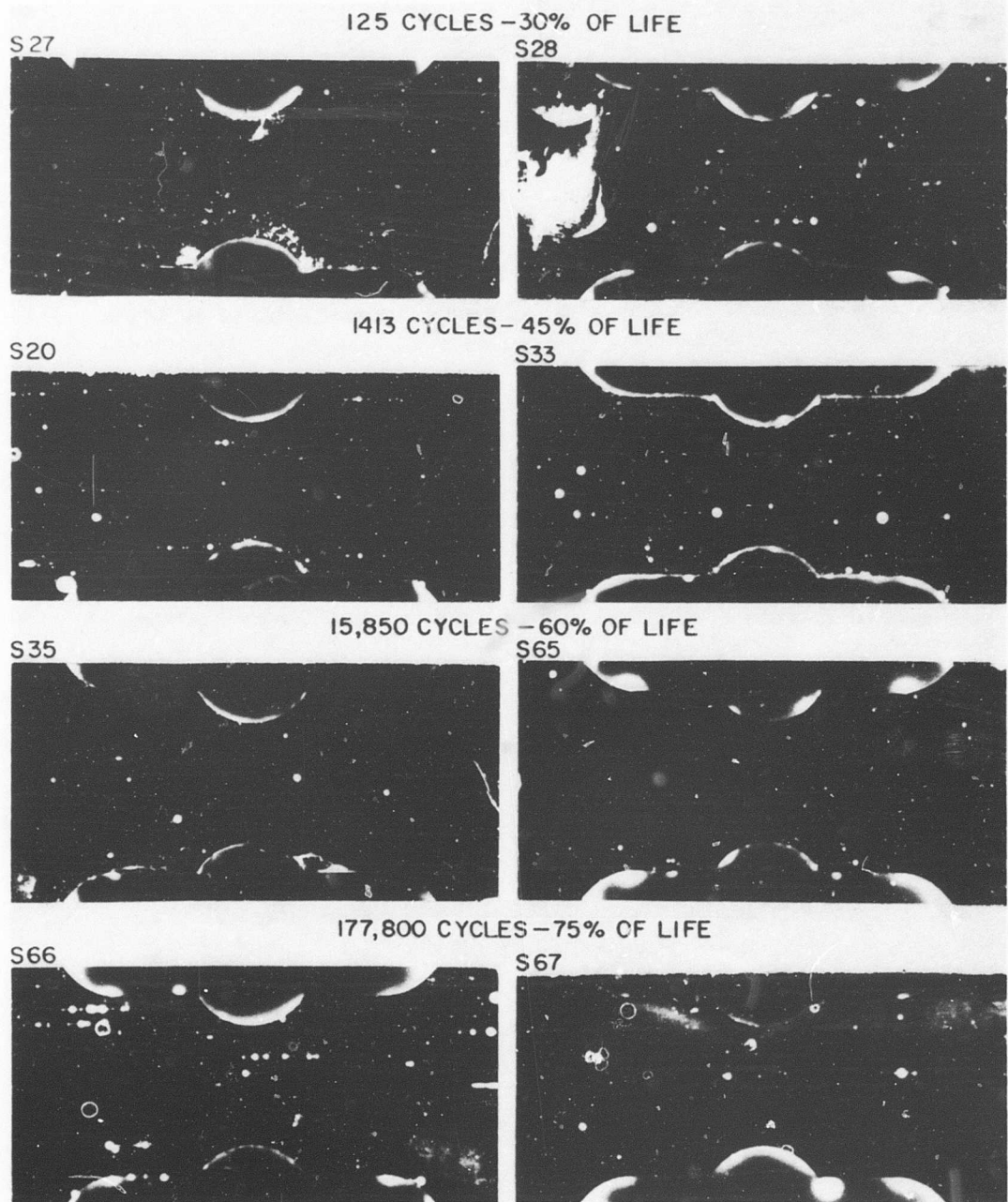


Figure 29. 4130 Steel Specimens Tested to Fractions of Fatigue Life.

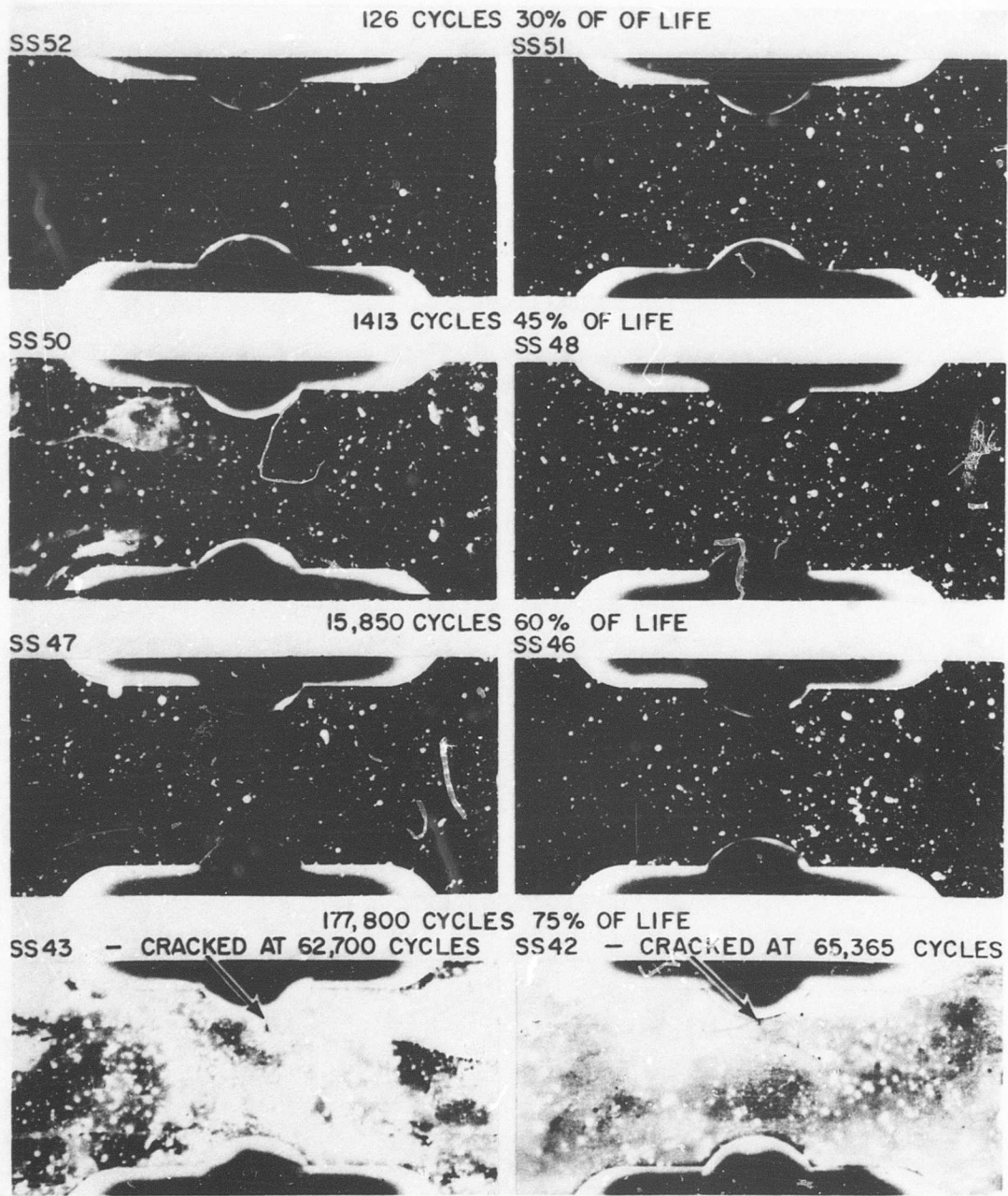
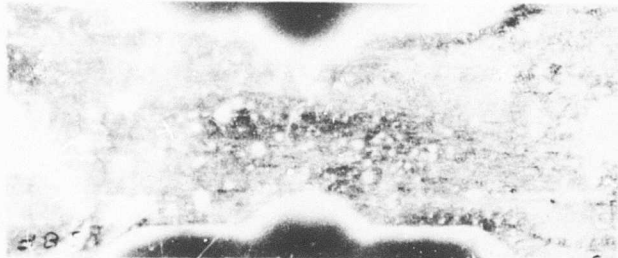


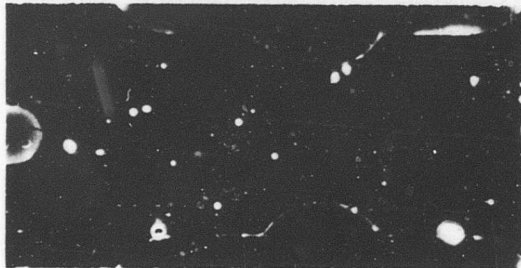
Figure 30. 301 Stainless Steel Specimens Tested to Fractions of Fatigue Life.

S 8
Front
Side



AFTER
KRYPTONATION
0 CYCLES

S 8
Front
Side



90 % OF FATIGUE LIFE
AFTER 1,995,000 CYCLES
AT 75 KSI

S 8
Front
Side



AFTER 10,357,000
CYCLES AT 75 KSI.
(ELONGATION
AT BOLT HOLE)

Figure 31. Autoradiographs of 4130 Steel Specimen Near Failure.

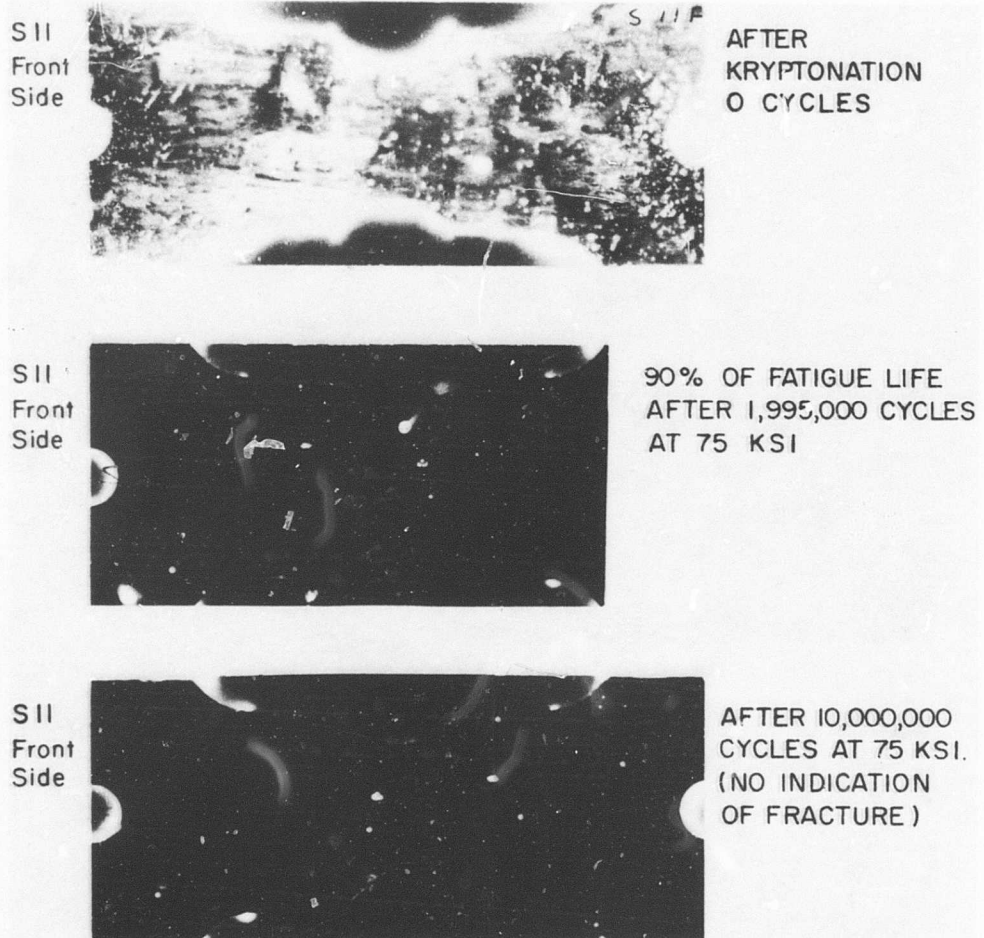
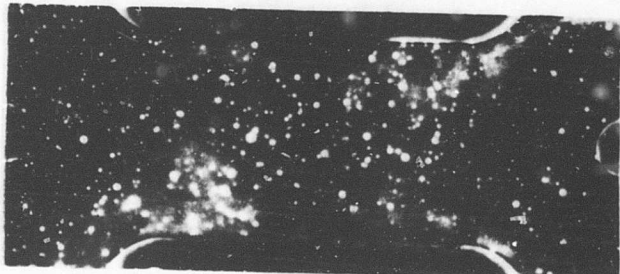


Figure 32. Autoradiographs of 4130 Steel Specimen Near Failure.

SS 49
Front
Side



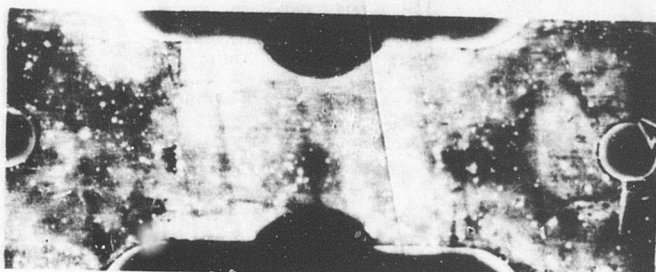
AFTER
KRYPTONATION
0 CYCLES

SS 49
Front
Side



90% OF
FATIGUE LIFE
1,995,000 CYCLES
AT 108 KSI

SS 49
Front
Side



AFTER
2,197,000 CYCLES
AT 108 KSI
(FRACTURE AT
BOLT HOLE)

Figure 33. Autoradiographs of 301 Stainless Steel Specimen Near Failure.

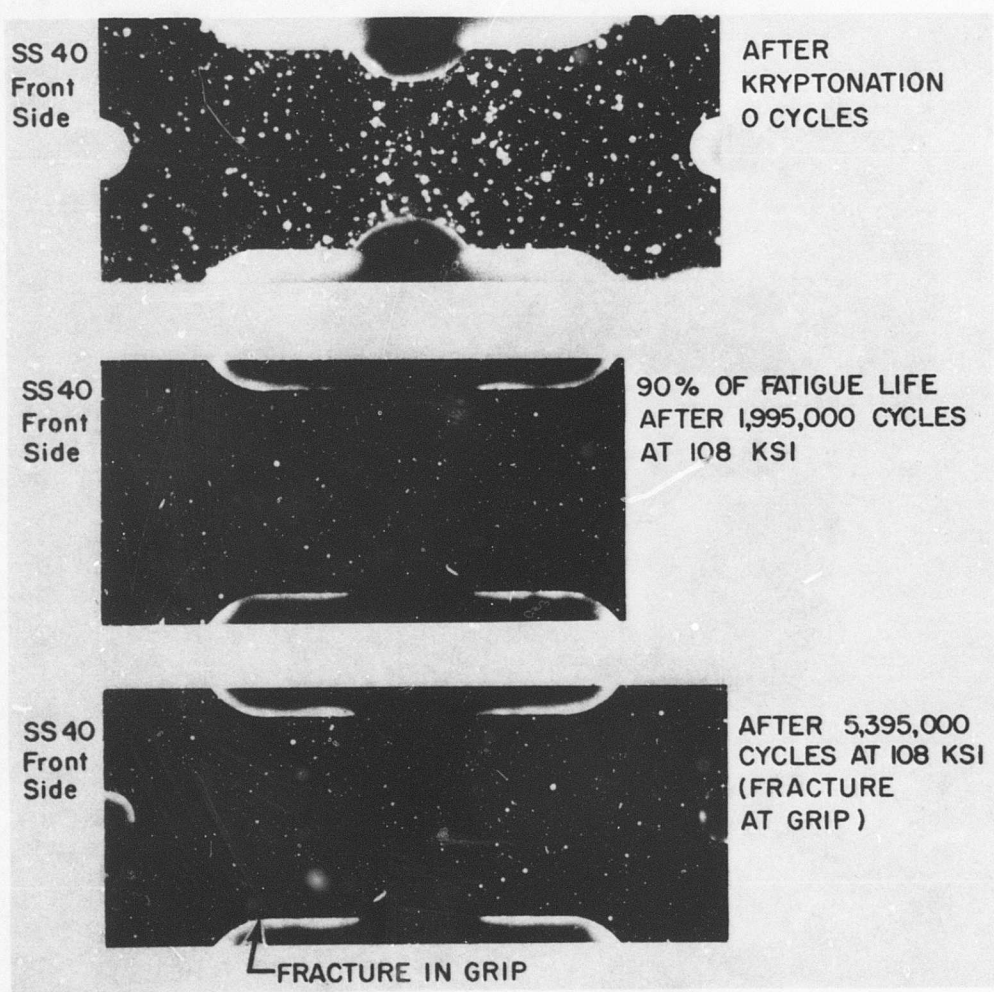


Figure 34. Autoradiographs of 301 Stainless Steel Specimen Near Failure.

indicate that krypton is released after fracture. This aspect of the study is discussed further in Subsection 4.2.1.

5.0 RESULTS AND CONCLUSIONS

By comparing the results of the statistical analysis of the kryptonated specimens with those of the unkryptonated specimens, it was determined in the preliminary phase of the study that the kryptonation method had no significant effect upon the fatigue lives of the materials at the stress levels examined. This result is significant in consideration of kryptonation as a potential performance evaluation sensor.

No strong correlation of stress fatigue and Kr-85 absorption or retention was obtained either by first fatiguing the three metals examined and then kryptonating them or vice-versa when Kr-85 retention as a function of outgassing time and Kr-85 retention and absorption as a function of fatigue history were examined. Certainly no predictive capability was found when kryptonation levels and fatigue life were compared. Weak or statistical correlation between Kr-85 absorption and retention and fatigue life was not examined in this study.

While neither radiometric nor autoradiographic measurements allowed fatigue history correlation within the scope of this study, several properties of kryptonated metals were determined. Krypton can detect small metal cracks due to stress fatigue by either pre- or post- kryptonation of 4130 normalized steel or 2024-T3 aluminum. While the limits of crack detection were not determined (that is, the smallest detectable crack), optically visible cracks of less than 2 mils width were detected. This was observed both in 4130 steel and in 2024 aluminum specimen which had first been fatigued to crack formation and then kryptonated, and in 4130 steel specimens which had first been kryptonated and then fatigued to crack formation. In the former case, cracks were indicated by high relative Kr-85 intensity and in the latter case by low relative Kr-85 intensity. Previous work has indicated that porosity of 10^3 A^0 diameter can be detected in certain other materials. These regions were noted as Kr-85 concentration points in their particular autoradiographs.

The 4130 steel specimens, which had been first kryptonated and then fatigued to near failure with crack formation occurring or to failure, showed a large loss of Kr-85 from the cracked or completely failed region. This was indicated in Figures 16 and 17. Of qualifying significance is the fact that this result did not occur until one week after the fatiguing process was over.

An undetermined sensitivity to stress was exhibited by 301 half hard stainless steel which had been first kryptonated and then fatigued. Radiometric measurements made during the fatigue cycling process indicated a loss of up to 50% of initial activity after the first application of a stress in the range of 112.5 to 117 Ksi (Figures 13, 14, and 15). This activity loss occurred after one stress application, with no significant decrease from this new activity level after 10^5 repetitions of the same stress. The autoradiographs, Figures 11 and 12, do not show a greater loss in the notched specimen region than elsewhere, but since the stress concentration factor is 1.36 and this maximum stress is only applied at the minimum cross-sectional area of the specimen, the autoradiographic results do not contradict the radiometric results.

The kryptonated 2024 aluminum was found to contain about 90% of the Kr-85 activity within its oxide layer by radiometric measurements made during polishing of the surface. The remaining 10% of activity was lost after two days.

Unclassified

Security Classification

DOCUMENT CONTROL DATA - R & D

(Security classification of title, body of abstract and indexing annotation must be entered when the overall report is classified)

1. ORIGINATING ACTIVITY (Corporate author)		2a. REPORT SECURITY CLASSIFICATION Unclassified
Industrial Nucleonics Corporation Columbus, Ohio		2b. GROUP
3. REPORT TITLE A STUDY TO DETERMINE IF A CORRELATION EXISTS BETWEEN METAL FATIGUE LIFE AND THE CAPABILITY OF THE METAL TO ABSORB OR RETAIN INERT GAS		
4. DESCRIPTIVE NOTES (Type of report and inclusive dates) Final Report		
5. AUTHOR(S) (First name, middle initial, last name) Albert J. Frasca		
6. REPORT DATE May 1969	7a. TOTAL NO. OF PAGES 81	7b. NO. OF REFS
8a. CONTRACT OR GRANT NO. DAAJ02-67-C-0021	8b. ORIGINATOR'S REPORT NUMBER(S) USAAVLABS Technical Report 69-34	
8c. PROJECT NO. Task 1F162203A43405	8d. OTHER REPORT NO(S) (Any other numbers that may be assigned this report)	
10. DISTRIBUTION STATEMENT 		
11. SUPPLEMENTARY NOTES	12. SPONSORING MILITARY ACTIVITY US Army Aviation Materiel Laboratories Fort Eustis, Virginia	
13. ABSTRACT The purpose of this study was to determine if a correlation exists between stressed metal fatigue and the ability of a metal to absorb or retain inert gas. Aluminum, stainless steel, and normalized steel samples were fatigued to percentages of their normal fatigue life and examined for preferential inert gas absorption in high fatigue regions. The inert gas was krypton, which was enriched with Kr-85, a radioactive tracer, for identification. The procedure was reversed for the same types of metals by allowing krypton absorption into the metals and examining for preferential release from subsequently fatigued areas. Autoradiography and radiometric analysis did not indicate any relationship between release or absorption of krypton and stress fatigue life with one exception; in the case of 4130 steel, limited results indicate that when Kr-85 absorption precedes fatigue, autoradiography and radiometric measurements can detect fatigue near failure. Peripheral results indicate that autoradiography is able to detect cracks in metals whether the inert gas absorption precedes or follows fatigue.		

DD FORM 1473 1 NOV 66
REPLACES DD FORM 1473, 1 JAN 64, WHICH IS
OBsolete FOR ARMY USE.

Unclassified

Security Classification

Unclassified

Security Classification

14. KEY WORDS	LINK A		LINK B		LINK C	
	ROLE	WT	ROLE	WT	ROLE	WT
Metal Fatigue						
Fatigue Life						
Inert Gas Absorption						
Krypton Absorption by Metal						
Autoradiography						

Unclassified

Security Classification

4662-69